Developing hierarchical density-structured models to study the national-scale dynamics of an arable weed.

Robert M. Goodsell[1] , Dylan Z. Childs[1] , Matthew Spencer[2], Shaun Coutts[3] , Remi Vergnon[1], Tom Swinfield[4], Simon A. Queenborough[5] , Robert P. Freckleton[1].

1. Department of Animal and Plant Sciences, University of Sheffield, UK, S10 2TN.
2. School of Environmental Sciences, University of Liverpool, L69 3GP.
3. Lincoln Institute for Agri-food Technology, University of Lincoln, LN2 2LG.
4. RSPB , Potton road, Sandy, Bedfordshire , SH19 2DL.
5. Yale School of Forestry & Environmental Studies, Yale University, New Haven, CT 06511, USA.

Submission type : Article

Word count: 7990

Corresponding author: Robert M. Goodsell, r.goodsell@sheffield.ac.uk

Department of Animal and Plant Sciences, University of Sheffield, UK, S10 2TN.

Running head: Modelling national scale plant dynamics.

Author contributions:

SQ & TS collected the data, RMG, RV, SC, DZC & RPF designed the study and carried out the analysis with support from MS. RMG wrote the manuscript with editorial advice from SC, DZC & RPF.

Abstract:

Population dynamics can be highly variable in the face of environmental heterogeneity, and understanding this variation is central in the study of ecology. Robust management decisions require that we understand how populations respond to management at a range of scales, and under a broad suite of conditions. Population models are potentially valuable tools in addressing this challenge. However, without adequate data, models can fail to produce useful results. Populations of arable weeds are particularly problematic in this respect, as they are widespread and their dynamics are extremely variable. Owing to the inherent cost of collecting data, most studies of weed population dynamics are derived from localized experiments under a small range of environmental conditions, limiting the extent to which variance in population dynamics can be measured. Density-structured models provide a route to rapid, large-scale analysis of population dynamics, and can expand the scale of ecological models that are directly tied to data. Here we extend previous density-structured models to include environmental heterogeneity, variation in management, and to account for inter-population variation. We develop, parameterize and test hierarchical density-structured models for a common agricultural weed, black-grass (*Alopecurus myosuroides*). We model the dynamics of this species in response to crop management, using survey data gathered over 4 years from 364 fields across a network of 45 UK farms. We show that hierarchical density-structured models provide a substantial improvement over their non-hierarchical counterparts. Using these models, we demonstrate that several alternative crop-rotations are effective in reducing weed densities. Rotations with high wheat prevalence exhibit the most severe infestations, and diverse rotations generally have lower weed densities. However, a key outcome is that in many cases the effect of crop rotation is small compared to the high variability arising from spatio-temporal heterogeneity. This result highlights the need to monitor and model population dynamics across large spatial and temporal scales in order to account for variation in the drivers

of plant dynamics. Our framework for data collection and modelling provides a means to achieve this.

Key words: Black-grass , weed control , Density-structured models , landscape ecology, agro-ecology.

Introduction:

Populations of many species are distributed across large spatial scales and are subject to highly variable environments. As a consequence, they can exhibit dynamics that are variable in both time and space, and depend on local conditions and context (Levin, 1992; Dunning *et al.*, 1995; Lundberg *et al.*, 2000; Coutts *et al.*, 2016). Managing populations in variable environments requires detailed knowledge of environment-driven spatio-temporal dynamics, whether the focus is on balancing natural resources and conservation (Tscharntke *et al.*, 2005; Flesch and Steidl, 2010; Damschen *et al.*, 2019), or eradicating problematic species (Freckleton *et al.*, 2000; Bianchi, Booij and Tscharntke, 2006; Ziska *et al.*, 2011). Understanding how populations respond to environmental drivers is essential for effective management, especially considering rapid rates of global change (Sutherland, 2006; IPCC, 2013; Sutherland *et al.*, 2013). However, gathering data of sufficient quality to encapsulate both the full range of population responses, and the associated environmental drivers, remains extremely challenging.

Gathering data over large scales is expensive and time consuming, leading to a trade-off between data extent and quality. As a result, ecological studies are typically reliant on intensive small-scale studies, and often only capture demographic variation at a few locations under relatively static conditions (Clutton-Brock *et al.*, 1996; Coulson *et al.*, 2001; Bremer and Jongejans, 2010; Dalgleish, Koons and Adler, 2010; Garnier *et al.*, 2018). These studies may produce high-quality data, but often fail to encompass the full range of conditions that populations experience (Forman, 1995; Miller *et al.*, 2004), and there is typically a lack of large-scale and detailed demographic data representing more than a few locations (Salguero-gomez *et al.*, 2015; Gurevitch *et al.*, 2016). Often, data from one or a small number of well-studied populations are used to generalise demography (Silvertown, Franco and Menges, 1996;

Salguero-Gómez *et al.*, 2016) with the assumption that this accurately depicts dynamics of populations over relevant scales (Burns *et al.*, 2010; Crone *et al.*, 2011).

However, generalisation of demography can be extremely problematic, as reliable extrapolation of demographic metrics is limited to local scales (Coutts *et al.*, 2016), and demographic parameters estimated for one population may be inappropriate for others (Che-Castaldo, Che-Castaldo and Neel, 2018). Generalising demographic traits is unreliable, partly due uneven sampling across space and phylogeny. Sampling bias exists across taxa, which confounds analysis as closely related species will often occupy ranges with similar environmental conditions (Coutts *et al.*, 2016).Similarly, local population models are also limited by the availability of suitable data, as temporal heterogeneity can make it difficult to obtain sufficient data to accurately estimate the environmental variance in key parameters (Cousens, 1995; Freckleton *et al.*, 2006).Without adequate parameterisation, demographic models can fail in the face of uncertainty (Freckleton *et al.*, 2008) and result in poor forecast accuracy (Crone *et al.*, 2013).

To effectively model population dynamics over large spatial extents, sampling must extend over multiple populations in order to accurately capture the variance and covariance in demographic parameters due to the environment (Crone *et al.*, 2011, 2013; Coutts *et al.*, 2016; Che-Castaldo, Che-Castaldo and Neel, 2018; Quintana-ascencio *et al.*, 2018; Damschen *et al.*, 2019). Density-structured modelling is a method that addresses this challenge by facilitating rapid data collection across multiple populations, whilst also permitting accurate characterisation of local population dynamics (Taylor and Hastings, 2004; Freckleton *et al.*, 2011, 2017; Queenborough *et al.*, 2011; Mieszkowska *et al.*, 2013; Tredennick, Hooten and Adler, 2017). Instead of a continuous measure of abundance, density-structured methods discretize local population numbers into ordinal density 'states' and model the probabilities of transition between these categories. This method addresses the problems faced by conventional

methods in two ways. First, it enables fast data collection over large spatial and temporal scales, because time-consuming counts of individual plants are replaced by rapidly-estimated density states. Second, model parameterisation is simplified because dynamics are summarised by transition matrices. Without the need for in-depth quantification of key demographic parameters, transition matrix models are more robust to numerical instability (which may be caused by parameters that are sensitive to environmental heterogeneity) and parameterisation error, both of which are potentially pathological for demographic models (Freckleton *et al.*, 2008, 2011; Freckleton and Stephens, 2009). Moreover, as these models are inherently empirical they facilitate collection of large amounts of data, which itself reduces the risk of estimation error. These features mean that density-structured models can be used to quantify a much wider range of responses to different stimuli which are directly underpinned by empirical data. Density-structured models enable studies to both encompass numerous locations over environmental gradients and accurately capture a large range of population responses to their environment (Freckleton *et al*. 2011).

Although density-structured population models are a promising technique, their application has been limited to the short term (Freckleton *et al.*, 2017) and often without accounting for location-specific effects (Taylor and Hastings, 2004; Mieszkowska *et al.*, 2013). In order for density-structured models to inform the management of widespread populations they need to account for variability across multiple scales. One of the limitations of density-structured models is that if there are S sites and K density-states, and transition probabilities differ between sites, then $S(K^2 - K)$ independent parameters need to be estimated, in order to measure the variation in population dynamics across all sites. This is because there are K^2 possible transtions between K density states in a single site, with sum-to-one constraints meaning that $K^2 - K$ parameters are required to characterise dynamics in one population.

134 Furthermore, it may be difficult to estimate transition probabilities if not all density classes are
135 observed at every site.

136 A powerful solution is to model the hierarchical organization within such data,
137 accounting for effects that reflect spatial or temporal dependence between parameters. We
138 define hierarchical models (also known as multi-level models) as models with multiple
139 variance components to allow partitioning of variance components belonging to different
140 groups (Gelman and Hill, 2007). Incorporating hierarchical effects into density-structured
141 models could improve the estimation of parameters of density-structured models in a number
142 of ways. First, hierarchical models can capture the variation in density-structured dynamics
143 across multiple populations, and simultaneously model the dynamics of individual populations
144 and landscapes (e.g. Freckleton *et al.*, 2017). Second, hierarchical models can deal with the
145 problem of estimating large numbers of parameters, for which there is little information,
146 through partial-pooling (Gelman and Hill, 2007), allowing all the data to inform the estimates
147 for each population. In the context of density-structured models, this benefit is potentially an
148 important advance given the likely need to estimate large numbers of parameters.

149 In this paper we develop hierarchical density-structured models for populations of an
150 arable weed subject to a range of different management regimes distributed across a landscape.
151 The threat to arable farming posed by weeds is escalating due to evolved resistance to multiple
152 herbicides, that makes them increasingly difficult to manage (Moss and Clarke, 1994; Powles
153 and Yu, 2010; Moss *et al.*, 2011; Hicks *et al.*, 2018; Jasieniuk, Brûlé-babel and Morrison,
154 2018), as well as exacerbated risks of invasion due to climate change (Dukes and Mooney,
155 2008; Peters, Breitsameter and Gerowitt, 2014).

156 It is particularly difficult to model arable weeds for several reasons. First they often
157 occur in complex and highly fragmented landscapes, existing as small populations in fields that

158 are subject to variable management practices (Wiese *et al.*, 1997; Mack *et al.*, 2000; Tilman *et*
159 *al.*, 2001; Walker *et al.*, 2005). Second, weeds are subject to very high levels of control, with
160 populations often close to an extinction threshold, making population dynamics potentially
161 numerically unstable (Freckleton *et al.* 2008). Finally, many demographic parameters are
162 extremely difficult to estimate from field data, due to population-specific variation in
163 environmental variables such as soil, climate, and crop varieties, which can lead to extreme
164 variability in dynamics (Cardina *et al.*, 1997; Wallinga *et al.*, 1999; R. P. Freckleton and
165 Watkinson, 2002; Freckleton and Stephens, 2009; Lima, Navarrete and González-Andujar,
166 2012; Lutman *et al.*, 2013). The consequence is that weed population dynamics can be very
167 challenging to predict because data are typically limited to single populations (Gonzalez-
168 Andujar and Fernandez-Quintanilla, 1991; Buhler, 1999; Freckleton *et al.*, 2000; Buckley,
169 Briese and Rees, 2003; Colbach *et al.*, 2005, 2006; Metcalfe *et al.*, 2018). However, density-
170 structured methods have proved successful in monitoring and modelling these populations
171 using large-scale survey data (Taylor and Hastings, 2004; Freckleton *et al.*, 2011, 2017;
172 Queenborough *et al.*, 2011)

173 We develop hierarchical density-structured models to estimate the effect of crop
174 rotation, an integral part of arable farming and weed management, on the population dynamics
175 of a common arable weed (Zacharias and Grube, 1984; Liebman and Dyck, 1993; Melander,
176 Rasmussen and Bàrberi, 2005). Specifically, we have two objectives. First, we aim to find the
177 best candidate hierarchical density-structured model for accurate characterisation of population
178 dynamics. Second, we apply these hierarchical density-structured models to a large-scale
179 dataset to examine the impact of crop rotation on weed dynamics. We then assess the impact
180 of alternative control strategies on one of Europe's most economically damaging weeds, black-
181 grass (*Alopecurus myosuroides)* (Moss and Clarke, 1994; Moss, Perryman and Tatnell, 2007a;
182 Moss *et al.*, 2011; Lutman *et al.*, 2013; Hicks *et al.*, 2018). To our knowledge, this study

represents one of the largest studies of weed population dynamics to date. Our models demonstrate extreme levels of between-field variability in weed density, relative to the effect of rotation, highlighting that quantification of spatio-temporal dynamics at such scales is vital in assessing the effectiveness of management.

Methods

Study system and survey

Densities of black-grass (*Alopecurus myosuroides* Huds., Poaceae) were recorded in a series of repeated surveys from 2007-2010. This data set includes 682 repeated field-scale surveys from 364 individual fields nested within 45 arable farms throughout the counties of Norfolk, Lincolnshire, and Bedfordshire in the UK. The density-structured survey method, detailed in Queenborough *et al*. (2011), involved repeated surveys of individual fields to map weed densities in a given survey year. Each field was divided up into a set (median = 438, IQR = 245) of 20 m x 20 m survey quadrats, predefined using a GPS system. Researchers walked the fields recording the densities at each quadrat as one of five categories: absent (A), low (L), medium (M), high (H), or very high (VH). These categories are roughly delineated by the quartiles of a lognormal density distribution, and were chosen based on previous studies that have critically evaluated the method to demonstrate high within and between-observer repeatability (Freckleton *et al*. 2011, Queenborough *et al*. 2011).

Modelling density-structured data

A density-structured model has the form:

$$\mathbf{n}(t+1) = \mathbf{T}\mathbf{n}(t), \qquad (1)$$

where **n** is a vector, of length K (where K is the number of density states), whose elements are the probabilities of each density state at time t, and **T** is a $K \times K$ column-stochastic matrix of transition probabilities:

$$\mathbf{T} = \begin{pmatrix} p_{11} & \cdots & p_{1K} \\ \vdots & \ddots & \vdots \\ p_{K1} & \cdots & p_{KK} \end{pmatrix}. \qquad (2)$$

The transition matrix, **T**, defines the population dynamics. Diagonal entries of **T** represent probabilities (p) that a quadrat in a given state will remain in that state for the next survey, and off-diagonals represent the transition between states between years. For example, p_{11} is the probability that a quadrat in state 1, will remain in state 1, and p_{12} is the probability that a quadrat in state 2 will transition to state 1. Equation (1) defines a first-order Markov chain model which can be used to predict future density state distributions. Detailed explanations and evaluations of density-structured models can be found in Freckleton *et al* (2011).

Analysing black-grass dynamics in response to crop rotation.

We investigated the effect of management on black-grass density by formulating density-structured models that simulate the impact of different rotations on weed density. In the context of weed populations crop-rotation involves cyclic environmental disturbance, under such circumstances, density-structured dynamics can be investigated using periodic models (Skellam, 1967; Lesnoff, 1999; Mertens, van den Bosch and Heesterbeer, 2002; Cushing and Henson, 2018). Population dynamics under different rotations can be modelled by changing the transition matrix in successive time steps in the Markov model (Appendix S1: Equation S9 & S10), and complex rotations can be modelled by changing the order of rotation-specific

transition matrices. The only condition is that the destination crop of the previous matrix is the initial crop of the next, i.e. if one matrix models the transitions from wheat to barley, the next matrix in the sequence must model the transitions from barley to the next crop.

Model fitting

To analyse the impact of environmental variability on population dynamics through rotations, we first constructed a set of models that accounted for field-level spatio-temporal effects on transition probabilities. We parameterised transition matrices for each field-year (i.e. a field observed in a given year) observed in subsets of data representing three rotations, wheat-to-wheat, wheat-to-oil seed rape (OSR) and OSR-to-wheat.

To estimate transition probabilities, we fitted latent variable ordered category logit models to our density-state data. These empirical models allowed easy conceptualisation of drivers of weed densities and flexible parameterisation. As such they can account for the variable dynamics present in weed populations (Gonzalez-Andujar and Hughes, 2000; Freckleton and Watkinson, 2002; Freckleton *et al.*, 2017) as they do not restrict transitions between non-adjacent categories (Agresti, 2012, pg 303).

In an ordered categorical model, the probability of observing a given category, *k,* at quadrat *i* is expressed in terms of a real-valued latent variable that reflects the true (unobserved) value. A linear predictor, η_i, is defined for each quadrat, which is constructed from the row-vector of J quadrat-specific explanatory variables, x_i , and the unknown column-vector parameter β_i . β_{ij} is therefore the effect of explanatory variable x_{ij} on n_i, such that:

$$\eta_i = \sum_{j=1}^{J} x_{ij}\,\beta_{ij} \qquad (3)$$

The constraint $\beta_{i1} = 0$ is enforced to allow identifiability, a common practice in such models (Agresti, 2012, pg 297). The ordering of categories in this model is then enforced through a set of *K*-1 (where *K* is the total number of categories), 'cut-point' parameters, c_i, where $c_1 < c_2 < \cdots c_{K-2} < c_{K-1}$ (Appendix S1: Equation S6). Although η is unobserved, we categorise outcomes according to the following rules, where Θ_{ik} gives the probability of observing state *k* at quadrat *i*.

$$\Theta_{i1} = 1 - logit^{-1}(\eta_i - c_1),$$

$$\vdots$$

$$\Theta_{ik} = logit^{-1}(\eta_i - c_{k-1}) - logit^{-1}(\eta_i - c_k), \qquad (4)$$

$$\vdots$$

$$\Theta_{iK} = logit^{-1}(\eta_i - c_{K-1}).$$

As there is potentially uncertainty when it comes to estimating parameters in these models with collinear observational data, we employed a Bayesian framework using the probabilistic programming language Stan (Stan Core Development Team 2017) to allow flexibility in parameterization and to account for this uncertainty. Full hierarchical and prior specifications are detailed in Appendix S1.

Alternative models

We constructed a series of five ordered category logistic regressions to compare alternative formulations for estimating transition probabilities in a hierarchical density-structured framework.

Model I – Global, non-hierarchical model

Model I is the formulation presented in equations (3) - (4). This model formed the baseline for all subsequent models and incorporated the effect of source state (i.e. density state of quadrat *i* at time *t*) as covariates $x_{i1} \dots x_{i5}$, which take the form of indicator variables. Equations (3) and (4) describe the model for the probability of observing state *k*, conditional on source state *j* Therefore p_{k1} in (2) is equivalent to Θ_k where $j = 1$ in equation (3). Model I was included in the analyses as a baseline reference for comparison, and had no hierarchical variance components. Models II-IV (summarised in Table 1) took different approaches to modelling the hierarchy present in our dataset.

Model II – Field-level intercept

The simplest model that accounts for between-field variability included a 'field' effect in the construction of the linear predictor. The scalar intercept term γ_f represented the field-level effect on the linear predictor within field *f*. Here the cut-point parameters $c_k \dots c_{K-1}$ remained as in equation (4):

$$\eta_{if} = \sum_{j=1}^{J} x_{ij}\,\beta_{ij} + \gamma_f \qquad (5) \quad \text{Model II}$$

Model III – Field-level source state effects

The logical extension of Model II was to permit more flexibility in the construction of the linear predictor by allowing the source-state effect to vary between fields. The global effect of source state β_{ij} and global cut-points $c_1 \dots c_{K-1}$, remained as in Model II. The source state effects

governing the probability of transition between density states, β_{ij}, are likely to be determined by the same process across a landscape. However environmental heterogeneity mean they may vary at the field level. To account for variance in field-level source state effects we estimated field-specific slopes for the effect of source density state. This can be expressed via an additional the column-vector parameter, γ_{jf}, which represents the effect of source state *j* in field *f* on η. The addition of γ_{jf} allowed the effect of source state to vary between fields and aimed to account for the various drivers that affect changes in black-grass densities between surveys:

$$\eta_i = \sum_{j=1}^{J} x_{ij}\left(\beta_{ij} + \gamma_{jf}\right) \qquad (6) \quad \text{Model III}$$

Model IV – Field-level cut-points

Many applications of hierarchical modelling use the approach we have outlined above, accounting for group-level variation by including a term for group-level effects in the construction of the linear predictor. In an ordered category logistic regression an alternative approach is to allow cut-point parameters to vary between each group (in our case field-years). The advantage of this method is greater flexibility in the estimation of transition probabilities, because the cut-points themselves, which control the conditional probability of an observation being in state 1*:K*, are able to vary between field. We implemented this method by estimating a set of cut-points for each field:

$$\Theta_{i1f} = 1 - logit^{-1}\left(\eta_i - c_{1f}\right),$$

$$\vdots$$

$$\Theta_{ikf} = logit^{-1}\left(\eta_i - c_{k-1f}\right) - logit^{-1}\left(\eta_i - c_{kf}\right), \qquad (7) \quad \text{Model IV}$$

314 ⋮

315 $$\Theta_{iKf} = logit^{-1}(\eta_i - c_{K-1f}).$$

316

317 *Model V – Field-level cut-points and field-level intercept*

318 The final model is a combination of models III and IV, with both random cut-points and a
319 random intercept included in the linear predictor. As such the linear predictor was the same as
320 in Model II, and the cut-point parameters were the same as in Model IV. For the purposes of
321 simplicity in model selection, we use data from the three most common rotations, wheat-to-
322 wheat, wheat-to-OSR and OSR-to-wheat, to compare our models using a variety of cropping
323 systems with different dynamics.

324

325 *Assessing predictive performance and posterior checks*

326 To assess model performance across the three rotational subsets selected for model fitting, we
327 used leave-one-out cross validation (LOO-CV) implemented in R package 'loo' version 1.1.0
328 (Vehtari, Gelman & Gabry 2016), using 'LOO-IC' (LOO information criterion) as a measure
329 of relative predictive error. We also visualized model performance via graphical posterior
330 predictive checks to assess any systematic prediction errors due to differences in
331 parameterisation between models. We simulated field scale density distributions from posterior
332 probabilities and compared them to the observed distributions in each corresponding field. We
333 compared the full distribution of density states as well as mean density states calculated for
334 each individual field. Although the density-states are categorical variables they delineate the
335 true underlying continuous distribution of black-grass, the mean density-state is therefore

approximately proportional to the geometric mean of the true abundance and a useful measure for comparison.

Ecological analyses.

To explore the impact of spatio-temporal variability on weed dynamics across different crop rotations, we used our best performing model (Model IV) to fit ordered category logistic regressions to each of observed rotations in Figure 1. In each of these models we estimate 'field-year' matrices for the transitions observed in each field in a given year, so that each matrix incorporates both spatial and temporal variability in transition probabilities. For example, we parameterised 7 matrices from observed transitions in fields rotated from barley into wheat, and 38 matrices of wheat into barley. As the data are fragmented and often lack uninterrupted observations within a single field, we use permutations of field-level matrices within rotations to allow us to simulate and compare more complicated rotations than we observe in the data. To examine black-grass dynamics under various crop rotations and environmental contexts we conducted three analyses using density-structured models.

Asymptotic and transient dynamics

Given enough time, density-structured transition models (with primitive matrices) will always converge on a stable density structure for any given point in the rotation cycle, because the sum-to-one constraints ensure that the dominant eigenvalue of any transition matrix is always one (Caswell, 2001). A general approach to studying the dynamics of these models is to compare the stable density structures and the rates of convergence of different rotations. To investigate the dynamics of particular cropping alternatives we compared net transition matrices for a series of two-step rotations. The asymptotic dynamics of a two-step rotation,

analogous to running the Markov chain for a large number of iterations, can be examined via net transition matrices, defined as the product of two field-level matrices in a given rotation:

$$\mathbf{T}^{ij}{}_{\mathrm{ABA}} = \mathbf{T}^{j}{}_{\mathrm{BA}}\mathbf{T}^{i}{}_{\mathrm{AB}}, \qquad (8)$$

where subscripts *A* and *B* on $\mathbf{T}$ represent the sequence of crops modelled in each transition matrix, and superscript denotes the field. $\mathbf{T}^{ij}{}_{\mathrm{ABA}}$ is therefore the matrix modelling transition probabilities of weeds between density states during the rotation of crops *A* to *B* to *A*, with the superscript denoting the specific permutation of field-years *i* and *j*. Permutation of field-year matrices as in equation (8) is required as many crop sequences were unobserved within a single field. This allows the simulation and assessment of the impact of site-specific effects on weed densities across a larger subset of rotations (Mertens, van den Bosch and Heesterbeer, 2002; Mertens *et al.*, 2006). We generated every possible model of the form $\mathbf{T}^{ij}{}_{\mathrm{WBW}}$, where subscript *W* denotes a wheat crop, and *B*, denotes an intermediate crop (Table 2). We also parameterise models for continuous wheat ($\mathbf{T}^{ij}{}_{\mathrm{WWW}}$) and continuous barley ($\mathbf{T}^{ij}{}_{\mathrm{BBB}}$). For each of these rotations we generate net matrices from each possible permutation of field-level matrices, thus, for the wheat: barley: wheat example, there are 38 field-level wheat to barley matrices ($\mathbf{T}^{i}{}_{\mathrm{WB}}$) and 7 barley to wheat matrices ($\mathbf{T}^{j}{}_{\mathrm{BW}}$), making a total of 266 (38 × 7) net matrices ($\mathbf{T}^{ij}{}_{\mathrm{WBW}}$). For each net matrix we calculated two summary statistics that allowed us to examine the dynamics of different cropping systems.

The stable density structure $\mathbf{s}$, gives the proportion of sites in a field in each density-state at the asymptote of each rotation and is a measure of the distribution of overall population density. For each net matrix, $\mathbf{s}$ can be calculated from the leading eigenvector of a net transition matrix:

$$s_i = \frac{v_i}{\sum_{j=1}^{K} v_j}, \qquad (9)$$

where v_1 is the right eigenvector of the matrix, and *i* indicates the element. **s** is a *K* length vector representing the field-level density state distribution in terms of proportion of the field in each category. To summarise asymptotic dynamics, we calculate the mean density state from the stable density structure for each net matrix, i.e. the proportion of a population occupied by each state multiplied by the integer value (1-5) of each state category.

The rate of convergence to this structure is a measure of how quickly the population would reach equilibrium after a disturbance, and is governed by the relationship between the dominant and subdominant eigenvalues (noting that the dominant eigenvalue is 1):

$$\rho = \frac{\lambda_1}{\lambda_2} = \frac{1}{\lambda_2}, \qquad (10)$$

where λ_1 is the dominant eigenvalue and λ_2 is the second largest eigenvalue. ρ is the 'damping ratio' and gives a measure of sensitivity in the face of perturbation, or the rate at which a population will approach its stable density structure. The higher this ratio, the faster the convergence (Caswell 2001 , p95).

Short-term projections using two-step rotations

From an agronomic perspective, prediction of short-term dynamics is important because weed management objectives (e.g. leading to outcomes in terms of yield and profit) are typically measured on very short time scales. We therefore analysed population dynamics on timescales of two years (e.g. following Freckleton *et al.*, 2017). As with the asymptotic and transient

dynamic analyses we constructed models for all possible rotations starting and ending with wheat, as well as continuous rotations of barley and wheat. Simulating wheat to wheat transitions ensures that transitions are meaningful, firstly as the severity of an infestation can be judged against a common crop, but also because wheat is the most economically valuable crop in the UK (DEFRA, 2018). We made two-step projections for each possible combination of field-level matrices, for three initial starting densities (i.e. the density-state distribution of the field at the beginning of the simulation), and represented typically low (A = 0.8 , L = 0.2 , M = 0 , H = 0 , VH = 0), medium (A = 0.6 , L = 0.2 , M = 0.2 , H = 0 , VH = 0) and high (A = 0.3 , L = 0.2 , M = 0.2 , H = 0.2 , VH = 0.1) levels of black-grass. Thus, for the wheat-barley-wheat example, there are 266 matrices for a single initial density and 798 (266 × 3) outcomes in total. We compared the average outcome and distribution of each rotation from each initial starting density, as well as the relative change compared to wheat.

To deconstruct the effects of environment and management, we used a life-table response-experiment (LTRE) (Caswell, 1989, Caswell 2001 p258) to analyse the variation in the change in weed density between years due to local spatio-temporal effects (or field identity), initial densities, and rotation. This method uses the change in black-grass density from the two-step projections described above as the response variable in a linear mixed-effects model (e.g. Freckleton *et al*. 2017), to account for variation in population structure and intrinsic dynamics:

$$Y_{ifjk} = \alpha_0 + \mu_f^{(1)} + \mu_j^{(2)} + \mu_k^{(3)} + \epsilon_{ifjk}, \qquad (11)$$

$$\mu_f^{(1)} \sim N(0\,, \theta_1),$$

$$\mu_j^{(2)} \sim N(0\,, \theta_2),$$

$$\mu_k^{(3)} \sim N(0\,, \theta_3),$$

$$\epsilon_{ifjk} \sim N(0, \sigma),$$

In (13) Y_i is the change in mean density state between years for an individual simulation outcome i. Parameters $\mu_f^{(1)}, \mu_j^{(2)}, \mu_k^{(3)}$, represent the effects of matrix-pair f (i.e. the permutation of field-level matrices used in the projection), initial density j, and rotation k respectively. Variances associated with these parameters are represented by $\theta_{1,2,3}$, and ϵ and σ are the residual error and its associated variance. α_0 represents the global intercept and was set to 1 in this analysis. To evaluate the variance components of field-level matrix-pair, initial density, and rotation we estimate parameters $\mu_f^{(1)}, \mu_j^{(2)}, \mu_k^{(3)}$ as random effects. Although there were only three levels in initial density, it was estimated as a random effect for the sake of efficiency and still provides the estimate of the variance component as would be obtained from treating it as a fixed-effect.

Long-term dynamics: stochastic projections

To investigate the impact of rotational diversity and type of break crop on weed density in the context of spatio-temporal variability we implement a series of stochastic models:

$$\boldsymbol{n}(\mathrm{t}+1) = \mathbf{T}^{i}{}_{\mathrm{AB}}\boldsymbol{n}(t),$$

$$\boldsymbol{n}(\mathrm{t}+2) = \mathbf{T}^{j}{}_{\mathrm{BA}}\boldsymbol{n}(t+1), \qquad (12)$$

where $\mathbf{T}^{i}{}_{\mathrm{AB}}$ denotes the field-level matrix that models transitions between crop *A* and *B* in field *i.* Stochasticity is implemented through an *iid* lottery, so that the 'field-level' matrix for a particular step in a rotation is sampled randomly as an independent and identically distributed variable. For example, for rotation *AB*, $\mathbf{T}^{i}{}_{\mathrm{AB}}$ is selected randomly from all fields in rotation *AB*, and for rotation *BA*, $\mathbf{T}^{j}{}_{\mathrm{BA}}$, is selected randomly from all fields in rotation *BA*. Modelling

dynamics in this way allows us to construct complicated rotational strategies that incorporate the large scale spatio-temporal variation captured by our surveys. We project the density state forward 10 000 time steps (to ensure convergence) for every model described in Table 3, which includes rotations with multiple break crops. All models were started at a 'low' density distribution, and mean density states were calculated at each time-step. Across time series we then compared means, variances, and coefficients of autocorrelation, for a series of rotations with different break crops, and rotational diversity (measured as the proportion of the dominant crop, wheat, in a rotation). From this we examined overall rotational effects on black-grass density, variability, and whether observed densities are likely to persist year-to-year.

Results

Model fitting

Hierarchical models (Models II-V) that incorporate 'field-level' effects into the transition probability have better predictive accuracy than our non-hierarchical model (Figure 2a). All hierarchical models provide similar levels of predictive performance. LOO-CV provided the most support for the models that incorporate hierarchical effects through cut-point parameters. Models that only incorporated hierarchical structure in the linear predictor fared slightly worse than field-level cut-point models, whilst there was no difference between in the field-level cut-point model (IV) and the combined linear predictor / cut-point model (V). Rotational subsets of our data all displayed the same order of model preference, suggesting that each model performs similarly under different cropping systems (Appendix S1 : Figure S1).

Through comparing observed and predicted field-scale mean density states it is again apparent that hierarchical models provided a better fit to the data than our baseline model (Figure 2b). Although slight improvements in terms of root-mean-square error (RMSE) were

seen from Models IV and V compared to II and III, all hierarchical models have similar performance as in all cases the prediction error and 80% equal-tailed credible intervals were close to zero.

There were, however, notable differences in the predictive accuracy of the non-hierarchical models between rotational subsets. Variance in field-scale predictive error was much higher in fields rotating from wheat or OSR into wheat (Figure 2b panels 1 and 3), than from wheat into OSR (Figure 2b, panel 2). The lower RMSE resulting from the predictions of Model I was also accompanied by a slight tendency to overestimate field-scale density. This was not the case with the hierarchical implementations, where all models displayed smaller error and higher correlations between observed and predicted densities.

Hierarchical models had lower error across density-state distributions for the wheat to wheat rotation (Figure 2c), and similar trends were evident in the other rotational subsets (Appendix S1 : Figure S1). Models II and III tended to under-predict the frequencies of absent states within fields, whilst having higher error around the frequencies of low and medium states. Models IV and V, on the other hand, had error distributions in all states close to zero and exhibited little evidence of systematic prediction error in the estimation of density-state distributions (Figure 2b and c).

The composite rotational matrices demonstrate that fields of continuous wheat exhibited higher probability of transition into higher density states than continuous barley (Figure 3, row 1). An absent quadrat in continuous wheat had a 0.28 probability of being occupied by low densities of black-grass the next year, but when rotating from barley to barley the same transition was 0.11. A similar tendency was apparent in matrices that modelled rotations *into* wheat (Figure 3, row 3). For example, there was a 0.18 probability that a patch of ‘very high’ density black grass would remain in that state when rotating from peas to wheat.

503 Conversely, rotations into an intermediate crop (Figure 3, row 2) showed the bulk of the
504 transition probability into lower density states.

505 Analysis of transient and asymptotic dynamics revealed that rotated systems stabilised
506 faster but in general had slightly lower equilibrium densities (Figure 4a and b). Equilibrium
507 density states for continuous wheat were generally higher and more variable than in rotations
508 that included break crops or continuous barley (Figure 4a). Using barley or peas as a break
509 crop resulted in the highest equilibrium density for rotated systems, whilst potatoes have the
510 lowest (Figure 4a). Continuous barley produced lower equilibrium densities than all rotations
511 using break crops.

512 Populations of black-grass that had been subjected to a rotation demonstrated higher
513 damping ratios than cropping of continuous barley or wheat, (Figure 4b) and therefore faster
514 convergence on a stable state distribution. Faster convergence was generally accompanied by
515 lower equilibrium densities, with the exception of barley and pea rotations where the pairing
516 suggested faster convergence on higher equilibrium densities. Although generally high
517 damping ratios were paired with low equilibrium densities, there was considerable variability
518 in these relationships (Appendix S1: Figure S2 & S3).

519

520

521

522

523 *Short term dynamics: two-step rotation:*

524 There were clear but weak patterns in the effect of rotation on mean density state in short term
525 simulations. After two-step rotations, field-scale mean density states differed between, but
526 were highly variable within, each rotation (Figure 5a). Continuous wheat and, to a lesser extent,
527 continuous barley, showed sensitivity to the initial density, indicating that the effectiveness of

528 rotation as a management tool depended on the starting conditions. However, some rotations
529 seemed to be invariant to initial state, for example rotation into OSR produced the same
530 outcome regardless of initial conditions.

531 For most rotations low initial densities resulted in higher final densities (Figure 5b),
532 populations with medium initial densities tended not to change, and populations at high initial
533 densities saw drastic reductions. Relative to continuous wheat, populations at low initial
534 densities in rotations of beans and sugar beet offer low reductions, while OSR and barley
535 offered virtually no reduction. Conversely rotating to peas increased weed density. At higher
536 starting densities all rotations, except into peas, offer considerable reduction in relative density
537 state.

538 Within two-step rotations it was clear that spatio-temporal effects and initial density
539 (i.e. the field specific conditions) explained the most variation in final density state, whilst the
540 actual management intervention (rotation) was marginal in its contribution (Figure 6). Large-
541 scale spatial and temporal heterogeneity (i.e., inter-field scale variation) had a large effect on
542 the outcome of management. We estimated the variance in change in density due to the identity
543 of the pair of matrices used in the model (spatio-temporal effects) as 0.45, variance of the initial
544 density conditions as 0.44, and the variance of each of the rotations as 0.03, with a residual
545 variance of 0.08.

546

547

548 *Long-term dynamics: stochastic projections:*

549

550 Reducing the proportion of wheat in a rotation decreased overall black-grass density,
551 but variability between break crops is evident (Figure 7), and there is considerable variability
552 in the trajectories of weed density of rotations when increasing proportion of wheat. For

example potatoes increase steeply in mean density from wheat proportions of 0.6 to 0.75, whilst the same increases in barley rotations were shallower. There was noticeable variation in the effect of break-crop on outcome density (Figure 8a). Using potatoes as a break crop produced significantly lower overall black-grass density, whilst OSR and peas produced comparably high levels. Potatoes also produced significantly lower between year variability (Appendix S1 : Figure S4a), whilst OSR, peas and barley produced the highest levels of between year variability in black-grass densities. Similar trends were evident in the relationship between break crop and autocorrelation (Figure S4b).

Discussion

Density-structured models are a promising method to assess the impact of environmental drivers on population dynamics over large spatial scales. Hierarchical implementations of these models allow simultaneous modelling of local and landscape scale dynamics. Hierarchical density-structured models provided considerable improvement compared to non-hierarchical model performance in terms of point-wise predictive capacity. The key finding is that the most flexible models (Models IV & V) performed the best; they had the lowest error in terms of out-of-sample prediction, and next-to no systematic error in predicting field-scale density-state distributions. This result reflects the fact there is a large amount of among field variation in the data. These models incorporated field-level effects via hierarchical cut-points, which allows more flexibility and better predictive performance than models that account for field specific effects in the linear predictor. These more flexible models may also account for more variation in factors that act at the field scale such as observation error, (e.g. the effect of different developmental stages of the crop or observation conditions) (Queenborough *et al.*, 2011), or

578 the ecology of the system (e.g. the effect of crop condition on transition probabilities).
579 However, they will not account for quadrat-level observation, such as misclassification of
580 density states. How variation in the observation process and more subtle aspects of population
581 ecology affect outcome in hierarchical cut-point formulations should be considered when
582 fitting these models in future applications.
583
584
585
586 *Density-structured modelling framework*
587 This study provides evidence for the capability of hierarchical density-structured models for
588 interrogating landscape-scale datasets on population responses to management. Analysis of
589 asymptotic, transient and stochastic dynamics all consistently illustrated that populations
590 responded to management. Populations that are spread over large areas are naturally subject to
591 a wide range of environmental effects and, in this case, management practices, both of which
592 are both likely to contribute to the variability in control that we observed here. The variability
593 in these populations demonstrates the necessity of large-scale monitoring, as effective
594 management relies on our understanding of the responses of populations to controls across the
595 range of environmental contexts in which they exist. Crucially, our density-structured approach
596 provides the data and modelling tools that permit this.
597 An important recent conceptual advance has been the genesis of 'landscape
598 demography' (Gurevitch *et al.*, 2016) which has demonstrated the importance of
599 environmental heterogeneity for population dynamics, and the prevalence of scale
600 dependencies in ecology (Hui, Fox and Gurevitch, 2017; Quintana-ascencio *et al.*, 2018;
601 Damschen *et al.*, 2019). Although these approaches are still heavily reliant on intensive data
602 collection, they provide detailed information on the causes and consequences of demographic

603 variation across a landscape. Moreover, with the increase in accessibility of remote-sensing
604 technology it is becoming easier to collect expansive and high-resolution population-level data
605 which could begin to facilitate large-scale and in depth studies of population dynamics. Some
606 studies already demonstrate the promise of remote-sensing data in large-scale spatio-temporal
607 models (Conn *et al.*, 2015; Tredennick *et al.*, 2016). However, these studies rely on high quality
608 population assessment, which is often difficult to achieve with remotely-sensed data across
609 large spatial extents (Lambert *et al.*, 2018; Lambert, Childs and Freckleton, 2019), and spatio-
610 temporal models still remain computationally intensive compared to density-structured
611 approaches. Considering the importance of environmental heterogeneity that we have
612 highlighted, the computational and data intensive nature of most large-scale modelling
613 techniques will limit their utility to expedite management at the relevant scales. Density-
614 structured models are a useful component of the rapidly expanding set of tools in large-scale
615 ecology. They offer a good alternative to many more complex approaches to fulfil the need for
616 empirical studies of population dynamics across landscapes, managements, and environmental
617 gradients. Although useful alternatives to traditional approaches, density-structured models
618 may sometimes be unable to fully capture the underlying continuous dynamics of the
619 population (Freckleton *et al.*, 2011). As such we need to better understand the limitations of
620 density-structured models in order to bridge currents gaps in our knowledge of their ability to
621 model a range of complex dynamics.
622
623 *Management implications:*

624 Predicting the densities of weeds in the context of real-world environmental variability is vital
625 to understanding the effects of management. Diversifying management options is necessary to
626 maintain control of arable weeds, with increasing emphasis needed on non-chemical options
627 (Chauvel *et al.*, 2001; Hicks *et al.*, 2018). Interrogation of large-scale datasets on the ecology

628 of arable weeds provides a route to improve our understanding of the responses of weeds to
629 interventions at local and larger scales (Hicks *et al.*, 2018; Baucom and Busi, 2019; Comont *et*
630 *al.*, 2019).

631 Weed populations are inherently variable and there is a significant body of literature
632 dedicated to understanding the causes and consequences of this variability (Freckleton and
633 Watkinson, 1998, 2002; Gonzalez-Andujar and Hughes, 2000; Freckleton and Stephens, 2009).
634 Field-scale variation in weed density can have various origins. For example, persistent
635 seedbanks, soil type, and local climatic variables will all substantially impact on black-grass
636 populations throughout the season (e.g., Colbach *et al*., 2006, Metcalfe *et al*., 2018).
637 Monitoring and predicting highly variable dynamics is challenging, but the first step to tackling
638 the issue is capturing the range of responses exhibited by a population. Our models capture the
639 high inter-population variability across a national-scale and within all the cropping systems we
640 considered.

641 The considerable variation in black-grass density between fields, regardless of rotation
642 used, has implications for both the large-scale modelling and management of black-grass. High
643 levels of variability suggest that in some cases, any benefit from an applied control may be
644 overwhelmed by location-specific effects positively influencing black-grass growth
645 (Freckleton *et al*., 2017). Without the necessary data to model the drivers of the field-level
646 effects of black-grass dynamics, it becomes extremely difficult to predict outcomes for
647 individual populations. Additional covariates, such as climate (Lima, Navarrete and González-
648 Andujar, 2012; GarcÍa De León *et al.*, 2014), soil type (Colbach *et al.*, 2006; Metcalfe *et al.*,
649 2017, 2018), herbicide resistance status (Moss, Perryman and Tatnell, 2007b; Moss *et al.*,
650 2011; Hicks *et al.*, 2018) and more specific management options (Holst, Rasmussen and
651 Bastiaans, 2007; Harker and O'Donovan, 2013; Metcalfe *et al.*, 2017) are obvious areas where

652 the predictive performance of these models could be improved, and should form the basis for
653 future applications.
654
655 Despite high levels of variability, we have provided evidence for the effectiveness of rotation
656 for reducing weed infestations. Weed densities were related to different aspects of crop
657 rotation, with control varying by break crops and the proportion of wheat in a rotation. This
658 result agrees with the current research on how cropping systems can provide control of
659 problematic weeds (Zacharias and Grube, 1984; Liebman and Dyck, 1993; Chauvel *et al.*,
660 2001; Melander, Rasmussen and Bàrberi, 2005; Moss, Perryman and Tatnell, 2007b), and
661 demonstrates that this approach provides correct assessments of dynamics.
662
663 In our models, cropping continuous wheat resulted in high density, highly variable
664 infestations of black-grass that are likely to persist. Wheat is well known to be particularly
665 susceptible to black-grass (Hicks *et al*. 2018): due to overlapping germination profiles, control
666 is limited by the risk of damage to the crop itself (Thurston, 1964). Our simulations
667 demonstrated that many populations converged on medium densities, this suggests that
668 alternative managements for moderate weed infestations may only produce small long-term
669 changes, which emphasises the importance of transient metrics in future modelling efforts.
670 Although differences in weed observability in different crops may also contribute to some of
671 the periodic differences we see across rotations, we show that rotation decreased not only the
672 average density of black-grass, but also its variability and autocorrelation, suggesting that weed
673 populations will be more predictable and less likely to persist in rotated systems. Colonisation
674 of wheat fields via margins, farm machinery or crop seed are likely drivers of establishment of
675 weed populations, but it is unlikely that they contribute to the differences in density we observe

here, as black-grass typically sheds the majority of its seed before harvest and exists in low densities in field margins(Walsh *et al.*, 2017).

The benefits of rotational controls are widely appreciated in the literature and have various modes of action (Zacharias & Grube 1984, Liebman & Dyck 1993). Primarily, rotation allows opportunities to apply controls without risking damage to crops. As black-grass emergence usually occurs during autumn (Thurston, 1964; Moss, 1990), rotating into a spring crop (known as spring cropping) is often cited as an effective control measure. Spring cropping can reduce black-grass abundance by facilitating targeted herbicide application, seed bed preparation, and cultivation during a period where the field is empty of crop, but during the germination period of the weed (Moss & Clarke 1994, Chauvel *et al*. 2001, Moss *et al*. 2007, Lutman *et al*. 2013). Many of the cropping systems with the lowest black-grass densities from our analyses include spring crops. For example, broad-leaf crops such as sugar beet, beans and potatoes are generally planted in spring and are also resistant to grass-specific herbicides.

Control can also be achieved through direct and indirect competition for resources. Competitive cultivars such as barley or OSR can suppress weed populations through rapid accumulation of biomass and exclusion from nutrients and sunlight (Nicholas, 1991). We see reductions in black-grass density from crops often cited by farmers as competitive, namely OSR and barley (Lutman *et al.*, 2013). Compared to continuous wheat these crops showed noticeable reductions in density, but densities were generally higher than most alternatives. Some of the benefit of competitive cultivars, however, comes from resistance to yield penalties rather than reduction of seed return (Andrew, Storkey and Sparkes, 2015), which may have accounted for the previous popularity of OSR despite the continued abundance of black-grass. An important consideration for future modelling is balancing the costs of infestation and

controls. As wheat is the most valuable crop in the UK (DEFRA, 2018), rotations that reduce the prevalence of wheat will reduce income. However, this economic loss will have to be balanced against the potential loss due continued infestation, the viability of alternative crops, and costs of additional controls.

An important limitation of density-structured models in the context of weed management is that they can only accurately provide summary descriptions of field-level densities. Spatial structure is an important driver of population dynamics and this is especially true for weeds. Numerous studies have investigated how the role of spatial structure in weed populations influences the persistence, spread, and control of weed populations (Rew and Cousens, 2001; Holst, Rasmussen and Bastiaans, 2007; Metcalfe *et al.*, 2017; Somerville *et al.*, 2017; Gonzalez-Andujar, Perry and Moss, 2018). It is possible that the greater influence of field-level effects compared to rotational management in our simulations is partly due to specific spatial configurations of weeds within fields. Within field dynamics, demography and spatial structure are also important in dictating larger scale patterns of weed abundance (Cardina *et al.*, 1997; Freckleton and Watkinson, 2002). Incorporating information on spatial interactions and plant life cycles will, therefore, be an important step for extending the utility of density-structured models and has two distinct advantages. First, it will improve the overall predictive capacity of density-structured models, allowing more accurate descriptions of landscape-scale dynamics. Second, it will allow predictions of individual populations and planning of targeted and more efficient management options.

Monitoring, understanding, and predicting large-scale population dynamics is an essential step for effective management. We demonstrate that the use of a rapid and accessible survey methodology in conjunction with density-structured modelling can directly tie

empirical observations to predictions of landscape scale population responses to management and environmental heterogeneity. With these tools we show that the densities of an economically important weed were driven by rotational management, but all systems we studied were subject to high degrees of between-field variability in the degree of control. From this work we have demonstrated that development of integrated controls that are effective over a wide range of environmental conditions will be necessary to limit the detrimental effects of arable weeds. Perhaps more importantly, this study demonstrates that we must extend the scale of sampling in ecology in order account for environmentally driven variability in dynamics. Density-structured models are a useful tool in this endeavour and offer a route to achieve robust and inexpensive analysis of spatially extensive populations.

Acknowledgements

We would like to thank Simon Doxford, Kirsty Burnett, Ira Cooke, Tom Parker, Stuart Smith, and Elaine Booth for assistance with data collection, and Richard Hull for useful advice during writing.

References:

Agresti, A. (2012) *Categorical Data Analysis*. 3rd edn. Wiley Interscience.

Andrew, I. K. S., Storkey, J. and Sparkes, D. L. (2015) 'A review of the potential for competitive cereal cultivars as a tool in integrated weed management', *Weed Research*, 55(3), pp. 239–248.

Baucom, R. and Busi, R. (2019) 'Commentary Evolutionary epidemiology in the field : a proactive approach for identifying herbicide resistance in problematic crop weeds', *New Phytologist*, 223(3), pp. 1056–1058.

Bianchi, F. ., Booij, C. . and Tscharntke, T. (2006) 'Sustainable pest regulation in agricultural landscapes: a review on landscape composition, biodiversity and natural pest control', *Proceedings of the Royal Society B: Biological Sciences*, 273(1595), pp. 1715–1727.

Bremer, P. and Jongejans, E. (2010) 'Frost and forest stand effects on the population dynamics of Asplenium scolopendrium', *Population Ecology*, 52(1), pp. 211–222.

Burns, J. H., Blomberg, S. P., Crone, E. E., Ehrlén, J., Knight, T. M., Pichancourt, J. B., Ramula, S., Wardle, G. M. and Buckley, Y. M. (2010) 'Empirical tests of life-history evolution theory using phylogenetic analysis of plant demography', *Journal of Ecology*, 98(2), pp. 334–344.

Cardina, J., Johnson, G. A., Sparrow, D. H., Cardina, J. and Johnson, G. A. (1997) 'The Nature and Consequence of Weed Spatial Distribution', *Weed Science*, 45(3), pp. 364–373.

Caswell, H. (1989) 'Analysis of life table response experiments: Decomposition of effects on

776 population growth rate', *Ecological Modelling*, 46, pp. 221–237.
777 Caswell, H. (2001) 'Matrix population models', *2nd Edition, Sinauer Associates*.
778 Chauvel, B., Guillemin, J. P., Colbach, N. and Gasquez, J. (2001) 'Evaluation of cropping
779 systems for management of herbicide-resistant populations of blackgrass', *Crop*
780 *Protection*, 20(2), pp. 127–137.
781 Che-Castaldo, J., Che-Castaldo, C. and Neel, M. C. (2018) 'Predictability of demographic
782 rates based on phylogeny and biological similarity', *Conservation Biology*, 32(6), pp.
783 1290–1300.
784 Clutton-Brock, T. H., Stevenson, I. R., Marrow, P., MacColl, A. D., Houston, A. I. and
785 McNamara, J. M. (1996) 'Population Fluctuations, Reproductive Costs and Life-History
786 Tactics in Female Soay Sheep', *The Journal of Animal Ecology*, 65(6), p. 675.
787 Colbach, N., Busset, H., Yamada, O., Dürr, C. and Caneill, J. (2006) 'AlomySys: Modelling
788 black-grass germination and emergence, in interaction with seed characteristics, tillage
789 and soil climate: Evaluation', *European Journal of Agronomy*, 24(2), pp. 113–128.
790 Comont, D., Hicks, H., Crook, L., Hull, R., Cocciantelli, E., Hadfield, J., Childs, D.,
791 Freckleton, R. and Neve, P. (2019) 'Evolutionary epidemiology predicts the emergence
792 of glyphosate resistance in a major agricultural weed', *New Phytologist*, 223(3), pp.
793 1584–1594.
794 Conn, P., Johnson, D., Ver Hoef, J., Hooten, M. and London, J. (2015) 'Using spatiotemporal
795 statistical models to estimate animal abundance and infer ecological dynamics from
796 survey counts', 85(2), pp. 235–252.
797 Coulson, T., Cathpole, E., Albon, S., Morgan, B., Pemberton, J., Clutton-brock, T., Crawley,
798 M. and Grenfell, B. (2001) 'Age , Sex , Density , Winter Weather , and Population
799 Crashes in Soay Sheep', *Science*, 292(May), pp. 1528–1532.
800 Cousens, R. (1995) 'Can we Determine the Intrinsic Dynamics of Real Plant Populations ?',

Functional Ecology, 9(1), pp. 15–20.

Coutts, S. R., Salguero-Gómez, R., Csergő, A. M. and Buckley, Y. M. (2016) 'Extrapolating demography with climate, proximity and phylogeny: approach with caution', *Ecology Letters*, 19(12), pp. 1429–1438.

Crone, E. E. *et al.* (2011) 'How do plant ecologists use matrix population models?', *Ecology Letters*, 14(1), pp. 1–8.

Crone, E. E. *et al.* (2013) 'Ability of matrix models to explain the past and predict the future of plant populations', *Conservation Biology*, 27(5), pp. 968–978.

Cushing, J. M. and Henson, S. M. (2018) 'Periodic matrix models for seasonal dynamics of structured populations with application to a seabird population', *Journal of Mathematical Biology*. Springer Berlin Heidelberg, 77(6–7), pp. 1689–1720.

Dalgleish, H. J., Koons, D. N. and Adler, P. B. (2010) 'Can life-history traits predict the response of forb populations to changes in climate variability?', *Journal of Ecology*, 98(1), pp. 209–217.

Damschen, E. I., Haddad, N. M., Levey, D. J. and Warneke, C. (2019) 'Landscape heterogeneity is key to forecasting outcomes of plant reintroduction', 29(2), pp. 1–14.

DEFRA (2018) 'Agriculture in the UK', pp. 1–111.

Dukes, J. and Mooney, H. . (2008) 'Does global change increase the success of biological invaders?', 14(4), pp. 166–169.

Dunning, J. B. *et al.* (1995) 'Spatially Explicit Population Models : Current Forms and Future Uses', 5(1), pp. 3–11.

Flesch, A. D. and Steidl, R. J. (2010) 'Importance of environmental and spatial gradients on patterns and consequences of resource selection.', *Ecological applications : a publication of the Ecological Society of America*, 20(4), pp. 1021–39.

Forman, R. T. T. (1995) 'Some general principles oflandscape and regional ecology',

826 *Landscape Ecology*, 10(3), pp. 133–142.
827 Freckleton, R. P., Hicks, H. L., Comont, D., Crook, L., Hull, R. and Childs, D. Z. (2017)
828 'Measuring the effectiveness of management interventions at regional scales by
829 integrating ecological monitoring and modelling', *Pest Management Science*.
830 Freckleton, R. P. and Stephens, P. A. (2009) 'Predictive models of weed population
831 dynamics', *Weed Research*, 49(3), pp. 225–232.
832 Freckleton, R. P., Sutherland, W. J., Watkinson, A. R. and Queenborough, S. a (2011)
833 'Density-structured models for plant population dynamics.', *The American naturalist*,
834 177(1), pp. 1–17.
835 Freckleton, R. P., Sutherland, W. J., Watkinson, A. R. and Stephens, P. A. (2008) 'Modelling
836 the effects of management on population dynamics: Some lessons from annual weeds',
837 *Journal of Applied Ecology*, 45(4), pp. 1050–1058.
838 Freckleton, R. P. and Watkinson, A. R. (1998) 'How does temporal variability affect
839 predictions of weed population numbers?', *Journal of Applied Ecology*, 35(2), pp. 340–
840 344.
841 Freckleton, R. P. and Watkinson, A. R. (2002) 'Large-scale spatial dynamics of plants :
842 metapopulations , regional ensembles and patchy populations', *Journal of Ecology*, 90,
843 pp. 419–434.
844 Freckleton, R. P., Watkinson, A. R., Dowling, P. M. and Leys, A. R. (2000) 'Determinants of
845 the abundance of invasive annual weeds: community structure and non-equilibrium
846 dynamics', *The Royal Society*, 267(January), pp. 1153–1161.
847 Freckleton, R. P., Watkinson, A. R., Green, R. E. and Sutherland, W. J. (2006) 'Census error
848 and the detection of density dependence', *Journal of Animal Ecology*, 75(4), pp. 837–
849 851.
850 Freckleton and Watkinson (2002) 'Are weed population dynamics chaotic?', *Journal of*

Applied Ecology, 39(5), pp. 699–707.

GarcÍa De León, D., Freckleton, R. P., Lima, M., Navarrete, L., Castellanos, E. and González-Andújar, J. L. (2014) 'Identifying the effect of density dependence, agricultural practices and climate variables on the long-term dynamics of weed populations', *Weed Research*, 54(6), pp. 556–564.

Garnier, E. *et al.* (2018) 'Plant demographic and functional responses to management intensification: A long-term study in a Mediterranean rangeland', *Journal of Ecology*, 106(4), pp. 1363–1376.

Gelman, A. and Hill (2007) *Data Analysis Using Regression and Multilevel/Hierarchical Models*. Cambridge University Press.

Gonzalez-andujar, A. J. L., Perry, J. N. and Moss, S. R. (2018) 'Modelling Effects of Spatial Patterns on the Seed Bank Dynamics of Alopecurus myosuroides.', 47(6), pp. 697–705.

Gonzalez-Andujar, J. L. and Hughes, G. (2000) 'Complex dynamics in weed populations', *Functional Ecology*, 14(4), pp. 524–526.

Gurevitch, J., Fox, G. A., Fowler, N. L. and Graham, C. H. (2016) 'Landscape demography: population change and its drivers across spatial scales', 91(4), pp. 459–485.

Harker, N. and O'Donovan, J. (2013) 'Recent Weed Control, Weed Management, and Integrated Weed Management', *Weed Technology*, 45(5), pp. 290–301.

Hicks, H. L., Comont, D., Coutts, S. R., Crook, L., Hull, R., Norris, K., Neve, P., Childs, D. Z. and Freckleton, R. P. (2018) 'The factors driving evolved herbicide resistance at a national scale', *Nature Ecology and Evolution*. Springer US, 2(3), pp. 529–536.

Holst, N., Rasmussen, I. A. and Bastiaans, L. (2007) 'Field weed population dynamics : a review of model approaches and applications', pp. 1–14.

Hui, C., Fox, G. A. and Gurevitch, J. (2017) 'Scale-dependent portfolio effects explain growth inflation and volatility reduction in landscape demography', 114(47).

IPCC (2013) ‘Climate Change 2013: The Physical Science Basis. Contribution of Working Group I to the Fifth Assessment Report of the Intergovernmental Panel on Climate Change’, *Cambridge University Press, Cambridge*, p. 1535.

Jasieniuk, M., Brûlé-babel, A. L. and Morrison, I. N. (2018) ‘The Evolution and Genetics of Herbicide Resistance in Weeds P’, 44(1), pp. 176–193.

Lambert, J. P. T., Childs, D. Z. and Freckleton, R. P. (2019) ‘Testing the ability of unmanned aerial systems and machine learning to map weeds at subfield scales : a test with the weed Alopecurus myosuroides (Huds)’, (May).

Lambert, J. P. T., Hicks, H. L., Childs, D. Z. and Freckleton, R. P. (2018) ‘Evaluating the potential of Unmanned Aerial Systems for mapping weeds at field scales: a case study with Alopecurus myosuroides’, *Weed Research*, 58(1), pp. 35–45.

Lesnoff, M. (1999) ‘Dynamics of a sheep population in a Sahelian area (Ndiagne district in Senegal): A periodic matrix model’, *Agricultural Systems*, 61(3), pp. 207–221.

Levin, S. A. (1992) ‘The problem of pattern and scale in ecology’, 73(6), pp. 1943–1967.

Liebman, M. and Dyck, E. (1993) ‘Crop Rotation and Intercropping Strategies for Weed Management’, *Ecological Applications*, 3(1), pp. 92–122.

Lima, M., Navarrete, L. and González-Andujar, J. L. (2012) ‘Climate effects and feedback structure determining weed population dynamics in a long-term experiment’, *PLoS ONE*, 7(1), pp. 1–7.

Lundberg, P., Ranta, E., Ripa, J. and Kaitala, V. (2000) ‘Population variability in space and time’, *Trends in Ecology & Evolution*, 15(11), pp. 460–464.

Lutman, P. J. W., Moss, S. R., Cook, S. and Welham, S. J. (2013) ‘A review of the effects of crop agronomy on the management of *Alopecurus myosuroides*’, *Weed Research*, 53(5), pp. 299–313.

Melander, B., Rasmussen, I. A. and Bàrberi, P. (2005) ‘Integrating physical and cultural

methods of weed control — examples from European research Symposium Integrating physical and cultural methods of weed control.', *Weed Science*, 53(3), pp. 369–381.

Mertens, S. K., van den Bosch, F. and Heesterbeer, J. A. P. H. (2002) 'Weed populations and crop rotations: exploring dynamics of a structured periodic system', *Ecological Applications*, 12(4), pp. 1125–1141.

Mertens, S. K., Yearsley, J. ., Van Den Bosch, F. and Gilligan, C. A. (2006) 'Transient populations dynamics in periodic matrix models: methodology and effects of cyclic permutations.', 87(9), pp. 2338–2348.

Metcalfe, H., Milne, A. E., Hull, R., Murdoch, J. and Storkey, J. (2017) 'The implications of spatially variable pre-emergence herbicide efficacy for weed management', (November).

Metcalfe, H., Milne, A. E., Webster, R., Lark, R. M., Murdoch, A. J., Kanelo, L. and Storkey, J. (2018) 'Defining the habitat niche of Alopecurus myosuroides at the field scale', *Weed Research*, pp. 165–176.

Mieszkowska, N., Milligan, G., Burrows, M. T., Freckleton, R. and Spencer, M. (2013) 'Dynamic species distribution models from categorical survey data.', *The Journal of animal ecology*, 82(6), pp. 1215–26.

Miller, J. R., Turner, M. G., Smithwick, E. a. H., Dent, C. L. and Stanley, E. H. (2004) 'Spatial Extrapolation: The Science of Predicting Ecological Patterns and Processes', *BioScience*, 54(4), p. 310.

Moss, S. (1990) 'The seed cycle of Alopecurus myosuroides in winter cereals: a quantitative analysis', *Proc. EWRS Symposium, Integrated weed management in cereals.*, pp. 27–36.

Moss, S. R. and Clarke, J. H. (1994) 'Guidelines for the prevention and control of herbicide-resistant black-grass (Alopecurus myosuroides Huds.)', *Crop Protection*, 13(3), pp. 230–234.

926 Moss, S. R., Marshall, R., Hull, R. and Alarcon-Reverte, R. (2011) 'Current status of
927 herbicide-resistant weeds in the United Kingdom', *Aspects of Applied Biology*, 106, pp.
928 261–272.
929 Moss, S. R., Perryman and Tatnell, L. V. (2007a) 'Managing Herbicide-resistant Blackgrass
930 (Alopecurus Myosuroides): Theory and Practice', *Weed Technology*, 21(2), pp. 300–
931 309.
932 Moss, S. R., Perryman and Tatnell, L. V. (2007b) 'Managing Herbicide-resistant Blackgrass
933 (Alopecurus Myosuroides): Theory and Practice', *Weed Technology*, 21(2), pp. 300–
934 309.
935 Nicholas, J. (1991) 'Prospects for Weed Control Through Crop Interference', 3(1), pp. 84–
936 91.
937 Peters, K., Breitsameter, L. and Gerowitt, B. (2014) 'Impact of climate change on weeds in
938 agriculture: A review', *Agronomy for Sustainable Development*, 34(4), pp. 707–721.
939 Powles, S. B. and Yu, Q. (2010) *Evolution in Action: Plants Resistant to Herbicides, Annual*
940 *Review of Plant Biology*.
941 Queenborough, S. a., Burnet, K. M., Sutherland, W. J., Watkinson, A. R. and Freckleton, R.
942 P. (2011) 'From meso- to macroscale population dynamics: a new density-structured
943 approach', *Methods in Ecology and Evolution*, 2(3), pp. 289–302.
944 Quintana-ascencio, P. F., Koontz, S. M., Smith, S. A., Sclater, V. L., David, A. S. and
945 Menges, E. S. (2018) 'Predicting landscape- - level distribution and abundance :
946 Integrating demography , fire , elevation and landscape habitat configuration', (106), pp.
947 2395–2408.
948 Rew, L. J. and Cousens, R. D. (2001) 'Spatial distribution of weeds in arable crops: Are
949 current sampling and analytical methods appropriate?', *Weed Research*, 41(1), pp. 1–18.
950 Salguero-gomez, R. *et al.* (2015) 'The COMPADRE Plant Matrix Database : an open online

951 repository for plant demography', (103), pp. 202–218.
952 Salguero-Gómez, R., Jones, O. R., Jongejans, E., Blomberg, S. P., Hodgson, D. J., Mbeau-
953 Ache, C., Zuidema, P. A., de Kroon, H. and Buckley, Y. M. (2016) 'Fast–slow
954 continuum and reproductive strategies structure plant life-history variation worldwide',
955 *Proceedings of the National Academy of Sciences*, 113(1), pp. 230–235.
956 Silvertown, J., Franco, M. and Menges, E. (1996) 'Interpretation of elasticity matrices as an
957 aid to the management of plant populations for conservation', *Conservation Biology*,
958 10(2), pp. 591–597.
959 Skellam, J. G. (1967) 'Seasonal periodicity in theoretical population ecology', *Proceedings of*
960 *the 5th Berkeley Symposium on Mathematics, Statistics, and Probability*, 4, pp. 179–
961 205.
962 Somerville, G. J., Powles, S. B., Walsh, M. J. and Renton, M. (2017) 'How do spatial
963 heterogeneity and dispersal in weed population models affect predictions of herbicide
964 resistance evolution?', *Ecological Modelling*. Elsevier B.V., 362, pp. 37–53.
965 Sutherland, W. J. (2006) 'Predicting the ecological consequences of environmental change: A
966 review of the methods', *Journal of Applied Ecology*, 43(4), pp. 599–616.
967 Sutherland, W. J. *et al.* (2013) 'Identification of 100 fundamental ecological questions',
968 *Journal of Ecology*, 101(1), pp. 58–67.
969 Taylor, C. M. and Hastings, A. (2004) 'Finding optimal control strategies for invasive
970 species: a density-structured model for Spartina alterniflora', *Journal of Applied*
971 *Ecology*, 41(6), p. 1049.
972 Thurston, J. (1964) 'Germination of Alopecurus myosuroides Huds. (blackgrass).',
973 *Proceedings 7th Brit. Weed Control Conf.*
974 Tredennick, A. T., Hooten, M. B. and Adler, P. B. (2017) 'Do we need demographic data to
975 forecast plant population dynamics?', *Methods in Ecology and Evolution*, 8(5), pp. 541–

551.

Tredennick, A. T., Hooten, M. B., Aldridge, C. L., Homer, C. G., Kleinhesselink, A. R. and Adler, P. B. (2016) 'Forecasting climate change impacts on plant populations over large spatial extents', 7(October), pp. 1–16.

Tscharntke, T., Klein, A. M., Kruess, A., Steffan-Dewenter, I. and Thies, C. (2005) 'Landscape perspectives on agricultural intensification and biodiversity - Ecosystem service management', *Ecology Letters*, 8(8), pp. 857–874.

Wallinga, J., Grasman, J., Groeneveld, R. M. W., Kropff, M. J. and Lotz, L. A. P. (1999) 'Prediction of weed density: The increase of error with prediction interval, and the use of long-term prediction for weed management', *Journal of Applied Ecology*, 36(2), pp. 307–316.

Walsh, M. J. *et al.* (2017) 'Opportunities and challenges for harvest weed seed control in global cropping systems', *Pest Management Science*, 74(10), pp. 2235–2245.

Zacharias, T. and Grube, A. (1984) 'An Economic Evaluation of Weed Control Methods Used in Combination with Crop Rotation : A Stochastic Dominance Approach', *North Central Journal of Agricultural Economics*, 6(1).

Ziska, L. H., Blumenthal, D. M., Runion, G. B., Hunt, E. R. and Diaz-soltero, H. (2011) 'Invasive species and climate change : an agronomic perspective', *Climatic change*, pp. 13–42.

Table 1. Summary of candidate models with formulation of linear predictors and cut-point parameters.

Model	Description	Linear predictor	Cut-points
I	Global / non-hierarchical	$\eta_i = \sum_{j=1}^{J} x_{ij}\,\beta_{ij}$	Global
II	Field-level intercept	$\eta_i = \sum_{j=1}^{J} x_{ij}\,\beta_{ij} + \gamma_{if}$	Global
III	Field-level source state effect	$\eta_i = \sum_{j=1}^{J} x_{ij}\,(\beta_{ij} + \gamma_{ijf})$	Global
IV	Field-level cut-points	$\eta_i = \sum_{j=1}^{J} x_{ij}\,\beta_{ij}$	Field-level
V	Field-level cut-points & intercept	$\eta_i = \sum_{j=1}^{J} x_{ij}\,\beta_{ij} + \gamma_{if}$	Field-level

1011

1012

1013

1014

Table 2. Cropping systems included in the stochastic simulations. Includes the length of the rotation in years, the number of years a field spent in a break crop and the wheat dominance (proportion spent in wheat) of a rotation. Rotation denotes the sequence of wheat crops (W) and break crops (B), where B1 & B2 represent the first and second break crops in systems with two different break crops.

Break Crop	Length	No. of Break Years	Rotation	Wheat Dominance
Barley	1	1	B : B	0
	6	4	W : B : B : B : B : W	0.33
	5	3	W : B : B : B : W	0.4
	4	2	W : B : B : W	0.5
	3	1	W : B : W	0.66
	4	1	W : W : B : W	0.75
	5	1	W : W : W : B : W	0.8
Beans	3	1	W : B : W	0.66
	4	1	W : W : B : W	0.75
	5	1	W : W : W : B : W	0.8
Beet	3	1	W : B : W	0.66
	4	1	W : W : B : W	0.75
	5	1	W : W : W : B : W	0.8
OSR	3	1	W : B : W	0.66
	4	1	W : W : B : W	0.75

	5	1	W : W : W : B : W	0.8
Peas	3	1	W : B : W	0.66
	4	1	W : W : B : W	0.75
	5	1	W : W : W : B : W	0.8
Potatoes	3	1	W : B : W	0.66
	4	1	W : W : B : W	0.75
	5	1	W : W : W : B : W	0.8
Barley : Beet	2	2	B1 : B2	0
	6	4	W : B1 : B2 : B1 : B2 : W	0.33
	5	3	W : B1 : B2 : B1 : W	0.4
	4	2	W : B1 : B2 : W	0.5
	5	2	W : W : B1 : B2 : W	0.6
Barley : OSR	4	2	W : B1 : B2 : W	0.5
	5	2	W : B1 : B1 : B2 : W	0.6
Wheat	1	0	W : W	1

1020

1021

1022

Figure 1. A transition matrix illustrating the rotation space covered by models fit to observed data. Models were fit to each non-zero entry of this transition matrix. The top number in each cell is the number of fields, and the bottom number is the overall density-state observations in that rotation. The colour represents the number of fields in each observed rotation.

Figure 2. (a) LOO-IC scores calculated from leave-one-out cross validation for each model and rotational subset. Vertical bars are the standard errors around each LOO-IC estimate. (b) Field scale errors for mean density state by rotational subset. Hollow dots are median errors and vertical bars are 80% equal-tailed credible intervals. Numbers next to each median are the root-mean-square-error (RMSE) of the difference between predicted and observed densities. Individual coloured points represent difference between observed and predicted values for an individual field. Errors are relative to each rotational subset. 15 points were excluded from the extremes of Model I in this plot to allow clearer visualization but were included in calculations of RMSE. (c) Field-level error between observed and predicted frequencies for each density state category in the wheat-to-wheat subset. Black dots are median field-scale differences between predicted and observed frequencies of each density state across all fields, vertical bars are 80% equal-tailed credible intervals. Colours represent each of our 5 models, and individual coloured points represent the difference in observed vs density-state frequencies for individual fields. 43 points were removed from the extremes of Model I in this plot to allow clearer visualization.

Figure 3. Average transition probability matrices for given crop rotations. Matrices display the probability of transitioning from a state in year 1 (x axis) to any other state in year 2 (y axis). The darker the colour the higher the probability of transition. Numbers in each cell are

1049 the estimated probabilities. The first row are the matrices for continuous barley and wheat,
1050 the second row are matrices for rotations out of wheat, and the final row are rotations back
1051 into wheat.
1052
1053 Figure 4. Results from analysis of transient dynamics using damping ratios and mean density
1054 states from stable state distributions. Distribution of field level log damping ratios (a) and
1055 mean density states (b) for each rotation, and continuous crops of barley and wheat (C.barley
1056 & C.wheat). Hollow points are the median value across all permutations of net matrices, red
1057 and black bars are 90% and 50% equal-tailed credible intervals respectively.
1058
1059 Figure 5. (a) Mean density state distributions across all fields under rotations from wheat into
1060 potatoes, beans, sugar beet, OSR, barley and peas, as well as continuous barley (Po, Be, SB,
1061 OSR, Ba, Pe, & CBa), for three initial densities (low, medium and high). (b) Mean density
1062 state for model projections under rotations from wheat into potatoes, beans, sugar beet, OSR,
1063 barley and peas, as well as continuous barley (Po, Be, SB, OSR, Ba, Pe, & CBa), for three
1064 initial densities (low, medium and high).
1065
1066 Figure 6. Contribution to the variance in the difference between initial and final densities by
1067 Field ID/ matrix origin (first panel), initial density (second panel) and rotational control (third
1068 panel). Each point represents the size of the effect that variable had on the change in density.
1069 Points in the initial density panel are labelled accordingly (‘low’, ‘medium’, ‘high’). Points in
1070 the rotation panel correspond to density-structured models of continuous barley, potatoes,
1071 beans, sugar beet, OSR, barley, continuous wheat and peas respectively.
1072

Figure 7. Relationship between the proportion of wheat in a rotation and the mean density state across stochastic model projections. Individual points represent time-series averages for a model with a specific break crop/rotation at a specific proportion of wheat. Colours and shapes of each point represent the break-crop or combination of break crops used in each model. NB: the bottom left most point is two overlain points representing rotations of potatoes and continuous barley.

Figure 8. Mean density states, variance and Lag-1 autocorrelation in stochastic models with different break crops aggregated across levels of wheat dominance. Only models with a single break year and multiple levels of wheat dominance were included. Vertical bars represent two standard errors.

Figure legends:

Figure 1. A transition matrix illustrating the rotation space covered by models fit to observed data. Models were fit to each non-zero entry of this transition matrix. The top number in each cell is the number of fields, and the bottom number is the overall density-state observations in that rotation. The colour represents the number of fields in each observed rotation.

Figure 2. (a) LOO-IC scores calculated from leave-one-out cross validation for each model and rotational subset. Vertical bars are the standard errors around each LOO-IC estimate. (b) Field scale errors for mean density state by rotational subset. Hollow dots are median errors and vertical bars are 80% equal-tailed credible intervals. Numbers next to each median are the root-mean-square-error (RMSE) of the difference between predicted and observed densities. Individual coloured points represent difference between observed and predicted values for an individual field. Errors are relative to each rotational subset. 15 points were excluded from the extremes of Model I in this plot to allow clearer visualization but were included in calculations of RMSE. (c) Field-level error between observed and predicted frequencies for each density state category in the wheat-to-wheat subset. Black dots are median field-scale differences between predicted and observed frequencies of each density state across all fields, vertical bars are 80% equal-tailed credible intervals. Colours represent each of our 5 models, and individual coloured points represent the difference in observed vs density-state frequencies for individual fields. 43 points were removed from the extremes of Model I in this plot to allow clearer visualization.

Figure 3. Average transition probability matrices for given crop rotations. Matrices display the probability of transitioning from a state in year 1 (x axis) to any other state in year 2 (y axis). The darker the colour the higher the probability of transition. Numbers in each cell are the estimated probabilities. The first row are the matrices for continuous barley and wheat, the second row are matrices for rotations out of wheat, and the final row are rotations back into wheat.

Figure 4. Results from analysis of transient dynamics using damping ratios and mean density states from stable state distributions. Distribution of field level log damping ratios (a) and mean density states (b) for each rotation, and continuous crops of barley and wheat (C.barley & C.wheat). Hollow points are the median value across all permutations of net matrices, red and black bars are 90% and 50% equal-tailed credible intervals respectively.

Figure 5. (a) Mean density state distributions across all fields under rotations from wheat into potatoes, beans, sugar beet, OSR, barley and peas, as well as continuous barley (Po, Be, SB, OSR, Ba, Pe, & CBa), for three initial densities (low, medium and high). (b) Mean density state for model projections under rotations from wheat into potatoes, beans, sugar beet, OSR, barley and peas, as well as continuous barley (Po, Be, SB, OSR, Ba, Pe, & CBa), for three initial densities (low, medium and high).

Figure 6. Contribution to the variance in the difference between initial and final densities by Field ID/ matrix origin (first panel), initial density (second panel) and rotational control (third panel). Each point represents the size of the effect that variable had on the change in density. Points in the initial density panel are labelled accordingly ('low', 'medium', 'high'). Points in the rotation panel correspond to density-structured models of continuous barley, potatoes, beans, sugar beet, OSR, barley, continuous wheat and peas respectively.

Figure 7. Relationship between the proportion of wheat in a rotation and the mean density state across stochastic model projections. Individual points represent time-series averages for a model with a specific break crop/rotation at a specific proportion of winter wheat. Colours and shapes of each point represent the break-crop or combination of break crops used in each model. NB: the bottom left most point is two overlain points representing rotations of potatoes and continuous barley.

Figure 8. Mean density states, variance and Lag-1 autocorrelation in stochastic models with different break crops aggregated across levels of wheat dominance. Only models with a single break year and multiple levels of wheat dominance were included. Vertical bars represent two standard errors.

Figure S1. Field-level error between observed and predicted frequencies for each density state category for the wheat to OSR (top row) and OSR to wheat (bottom row) subsets. Hollow dots are median field-scale differences between predicted and observed frequencies of each density state across all fields, vertical bars are 80% equal-tailed credible intervals. Colours represent each of our 5 models, and individual coloured points represent the difference in observed vs density-state frequencies for individual fields.

Figure S2. The densities of (a) log of field-scale mean densities and (b) damping ratios for asymptotic & transient analyses of two-step rotations. The colour of each scale represents the corresponding value of each metric.

Figure S3. The relationship between damping ratio and the mean density of the stable state distribution of a particular matrix for each rotation in our analyses. The colour of each hex represents the log density of individual matrices at those values.

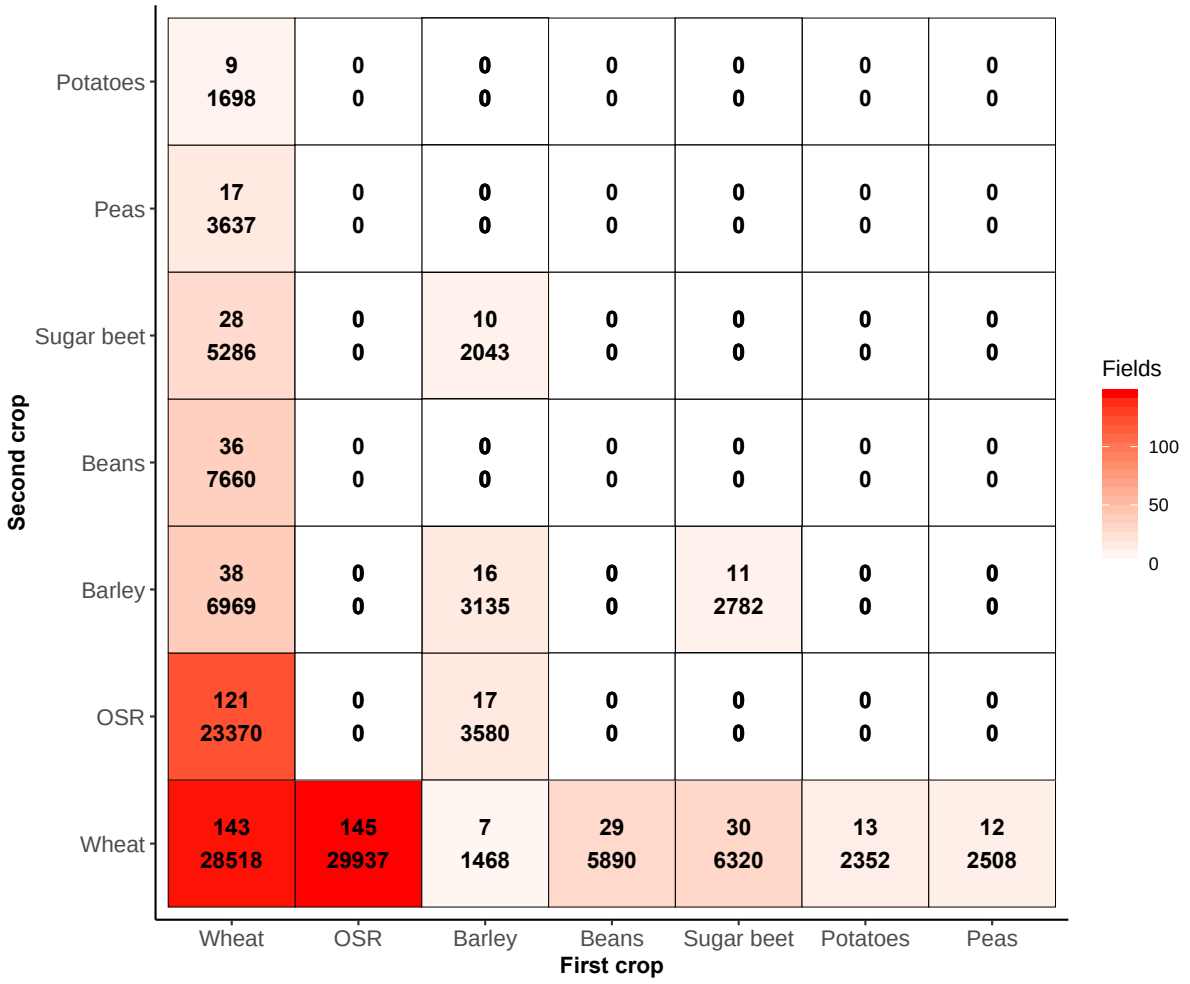
Potatoes
Peas
Sugar beet
Beans
Barley
OSR
Wheat
Second crop
9 1698
0 0
0 0
0 0
0 0
0 0
0 0
17 3637
0 0
0 0
0 0
0 0
0 0
0 0
28 5286
0 0
10 2043
0 0
0 0
0 0
0 0
36 7660
0 0
0 0
0 0
0 0
0 0
0 0
38 6969
0 0
16 3135
0 0
11 2782
0 0
0 0
121 23370
0 0
17 3580
0 0
0 0
0 0
0 0
143 28518
145 29937
7 1468
29 5890
30 6320
13 2352
12 2508
Wheat
OSR
Barley
Beans
Sugar beet
Potatoes
Peas
First crop
Fields
100
50
0

Figure 2.

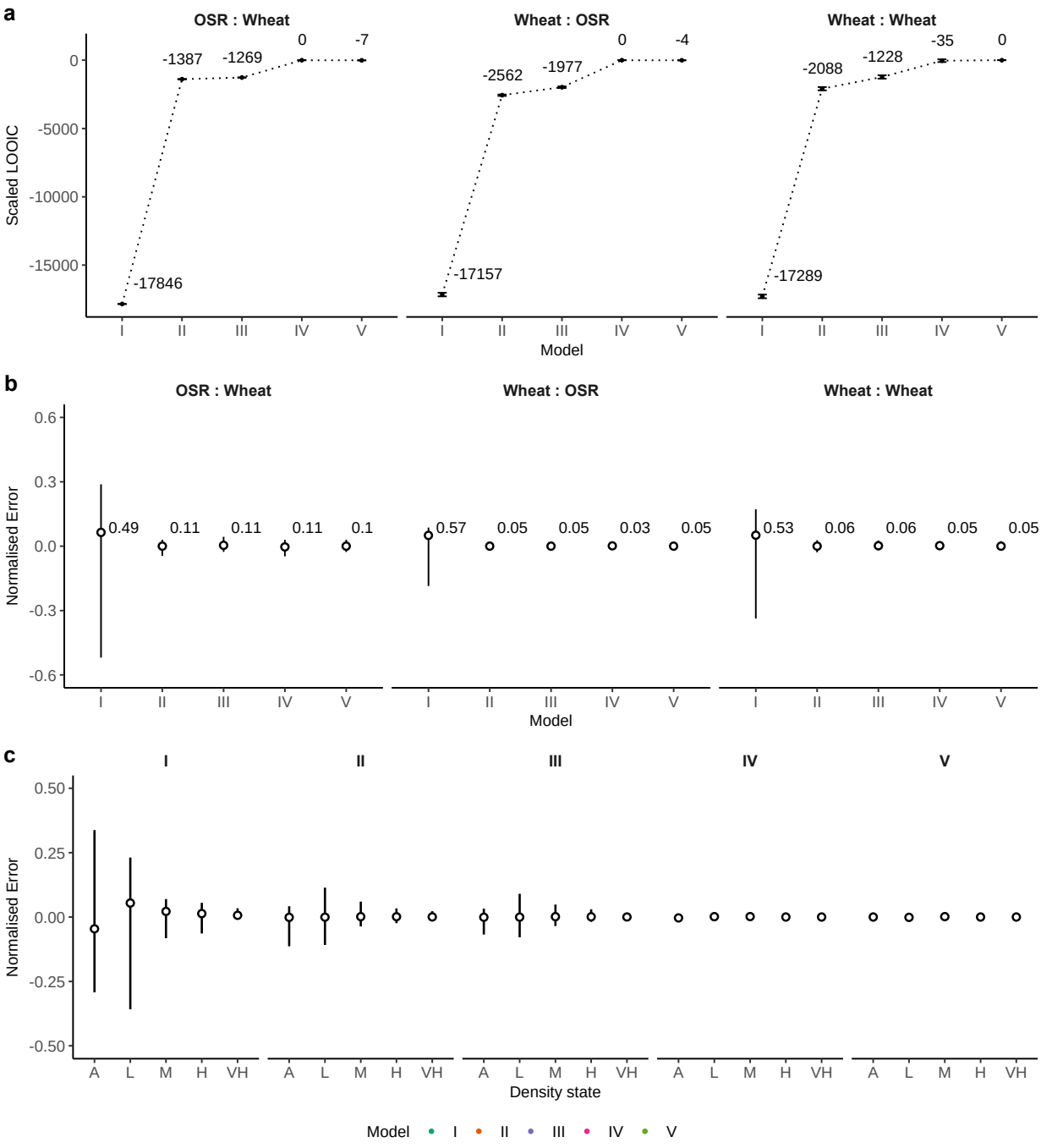
a
OSR : Wheat
Wheat : OSR
Wheat : Wheat
Scaled LOOIC
0
-5000
-10000
-15000
-1387
-1269
0
-7
-17846
-2562
-1977
0
-4
-17157
-2088
-1228
-35
0
-17289
I
II
III
IV
V
Model
b
OSR : Wheat
Wheat : OSR
Wheat : Wheat
Normalised Error
0.6
0.3
0.0
-0.3
-0.6
0.49
0.11
0.11
0.11
0.1
0.57
0.05
0.05
0.03
0.05
0.53
0.06
0.06
0.05
0.05
Model
c
I
II
III
IV
V
Normalised Error
0.50
0.25
0.00
-0.25
-0.50
A
L
M
H
VH
Density state
Model
I
II
III
IV
V

1180

1181 Figure 3.

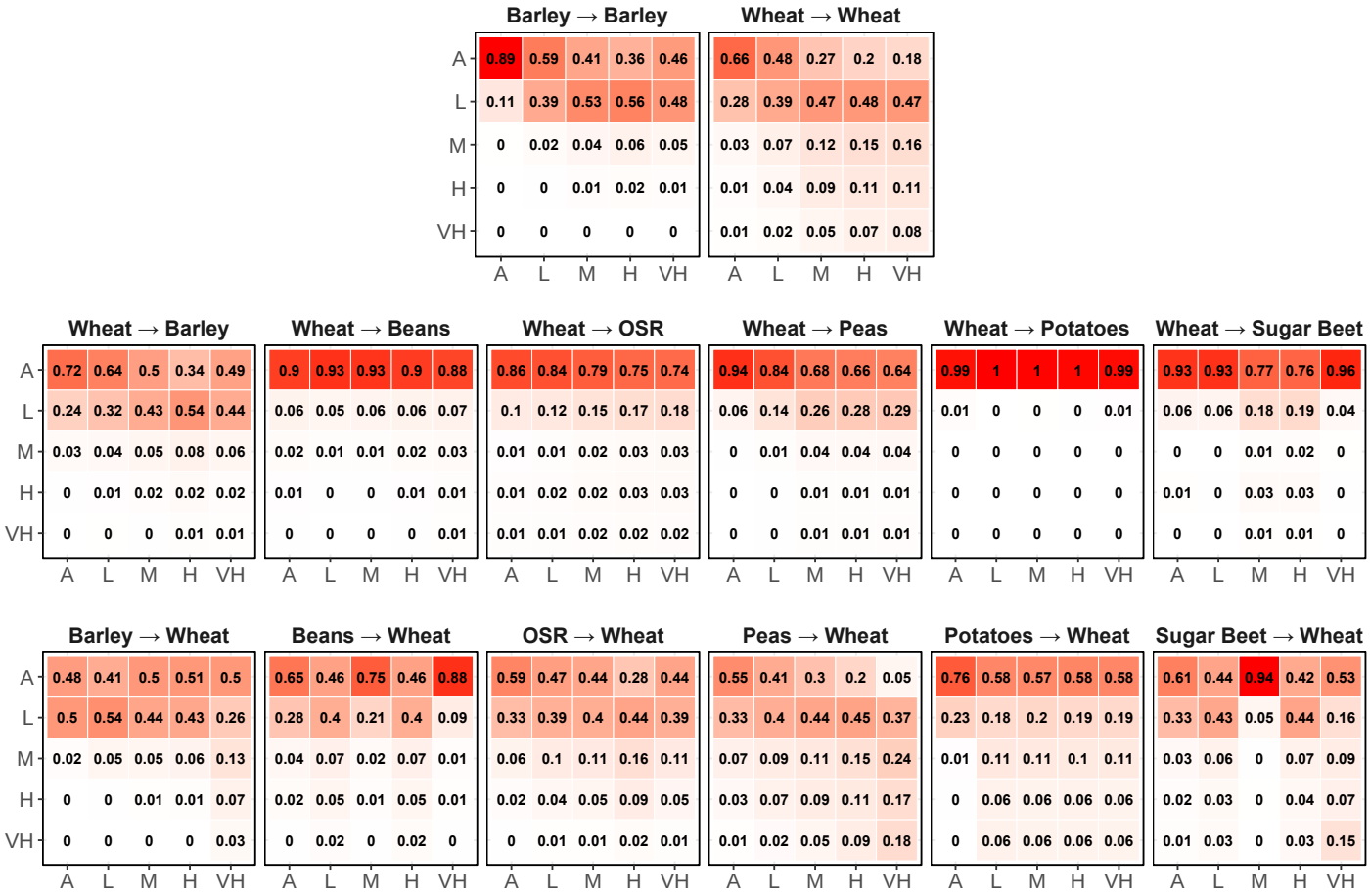

1182

1183 Figure 4.

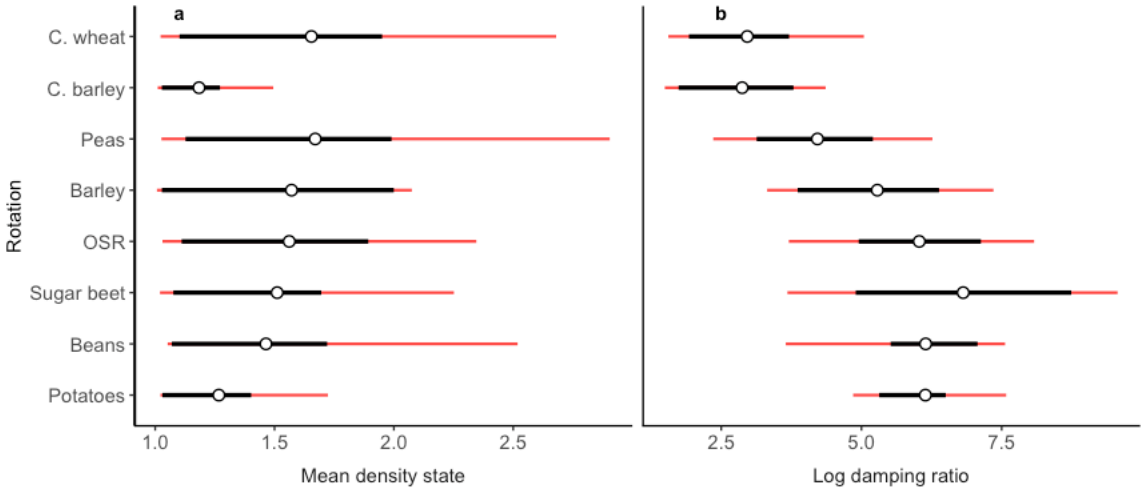

1184

1185 Figure 5.
1186

1187

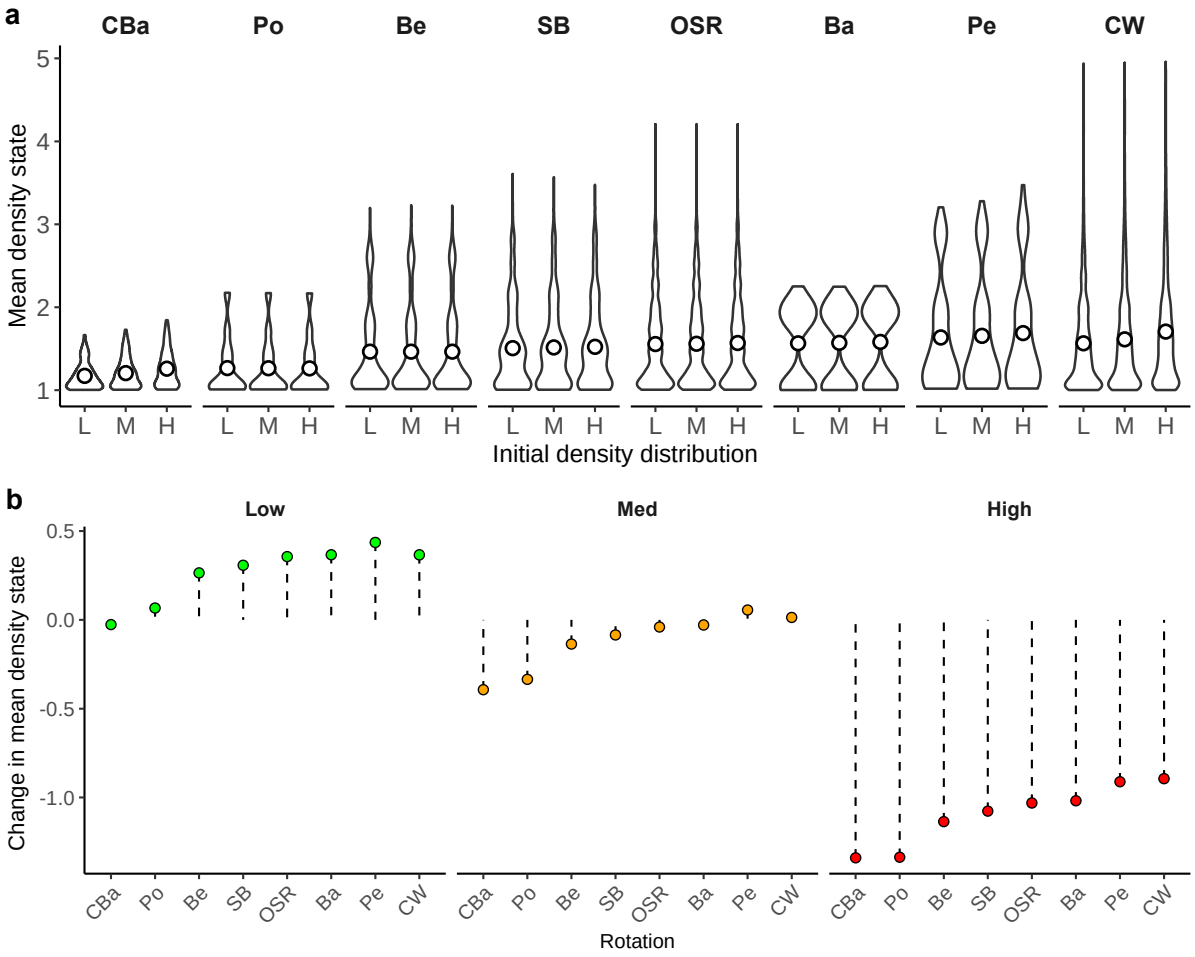

1188

1189 Figure 6.

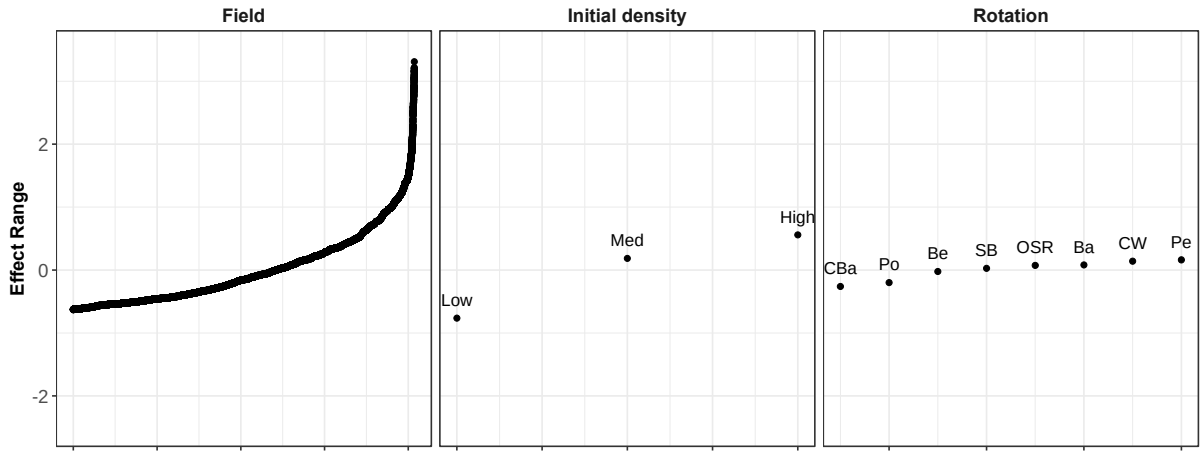

1190

1191

Figure 7.

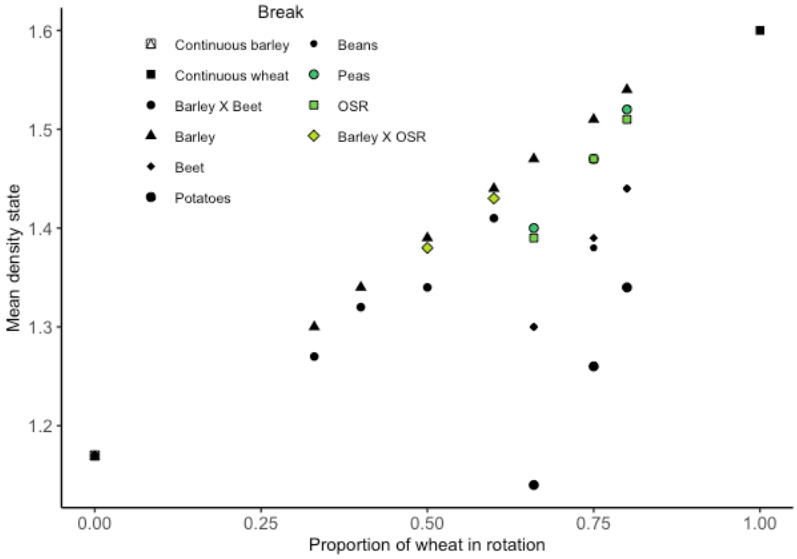
Break
Continuous barley
Continuous wheat
Barley X Beet
Barley
Beet
Potatoes
Beans
Peas
OSR
Barley X OSR
Mean density state
1.6
1.5
1.4
1.3
1.2
0.00
0.25
0.50
0.75
1.00
Proportion of wheat in rotation

1194 Figure 8.

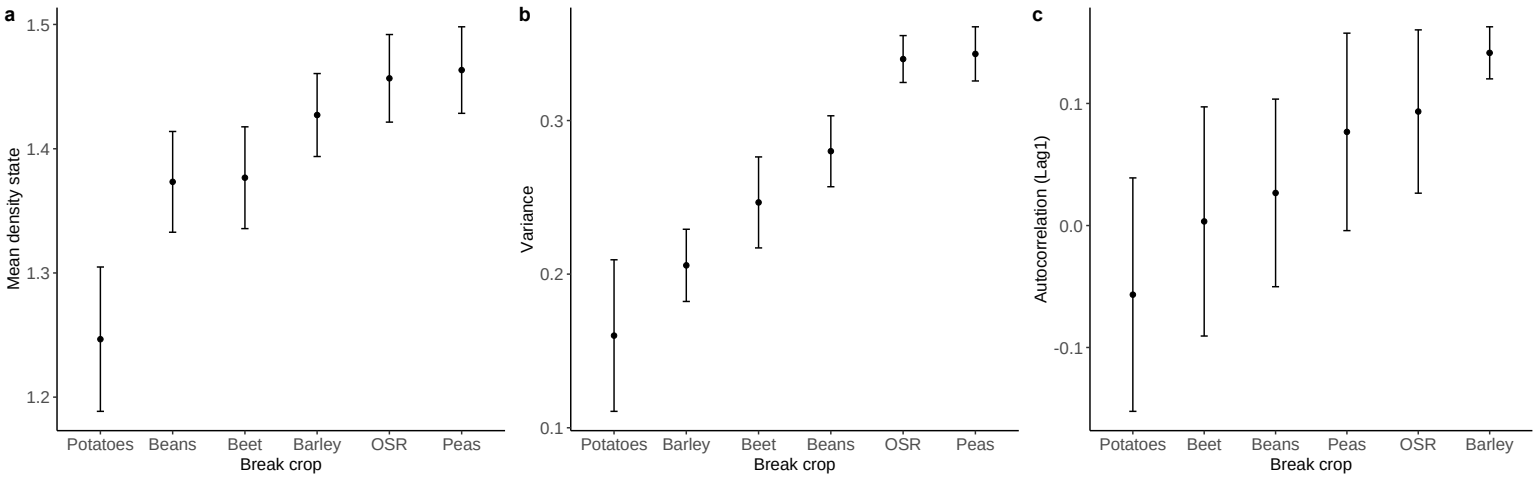

1195

1196

1197

1198

1199

1200

1201

1202

1203

1204

1205

1206

1207

1208

1209

1210

1211

1212

Figure S1

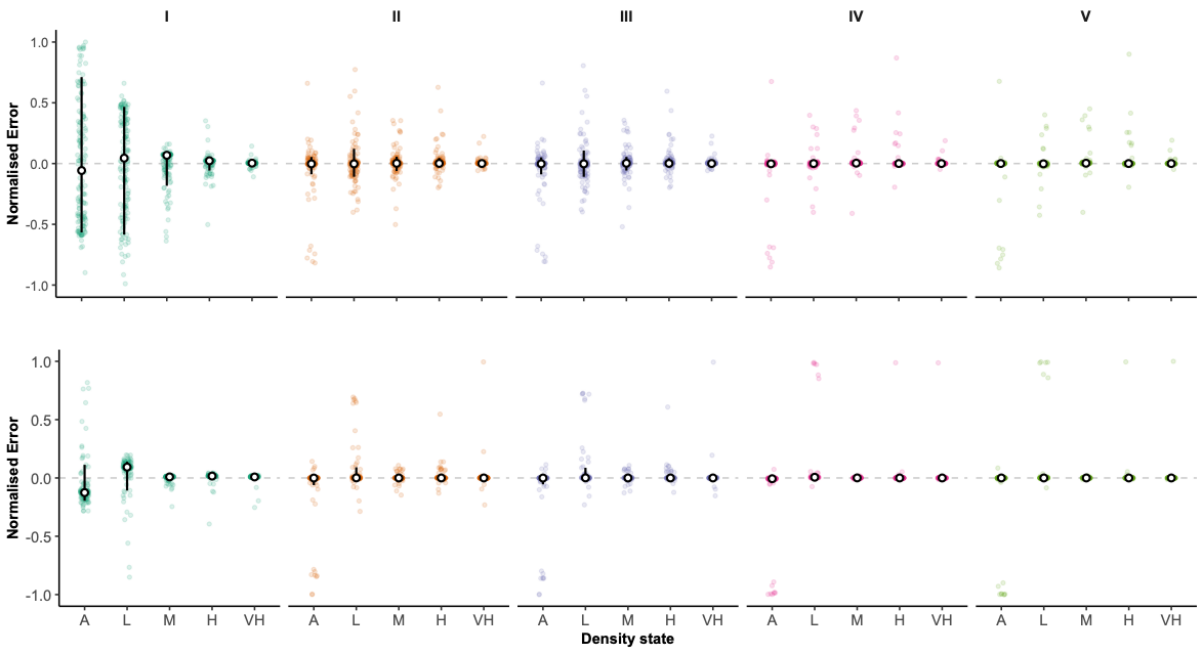
I
II
III
IV
V
Normalised Error
1.0
0.5
0.0
-0.5
-1.0
A
L
M
H
VH
Density state

Figure S2

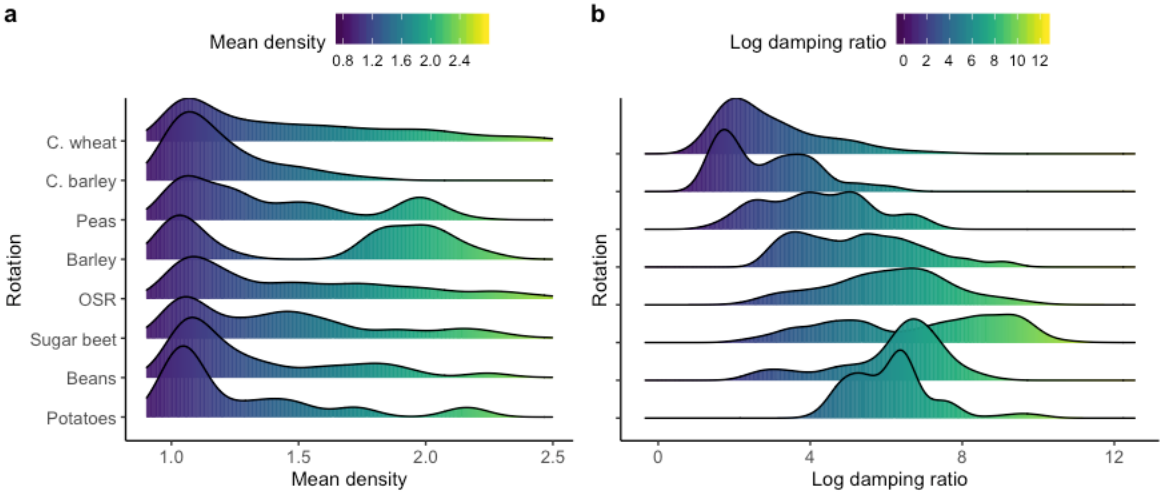
a
Mean density
0.8 1.2 1.6 2.0 2.4
C. wheat
C. barley
Peas
Barley
OSR
Sugar beet
Beans
Potatoes
Rotation
1.0
1.5
2.0
2.5
Mean density
b
Log damping ratio
0 2 4 6 8 10 12
Rotation
0
4
8
12
Log damping ratio

Figure S3.

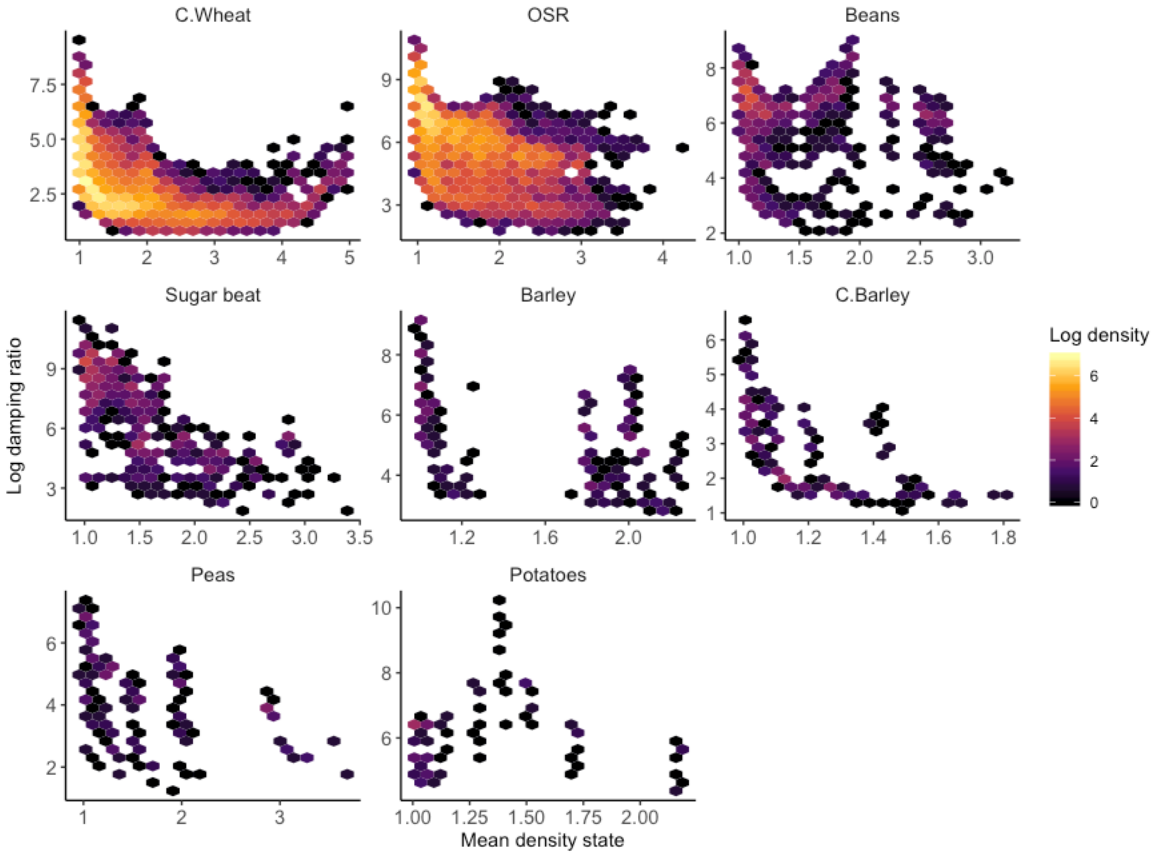
C.Wheat
OSR
Beans
Sugar beat
Barley
C.Barley
Peas
Potatoes
Log damping ratio
Mean density state
Log density

1264 Figure S4

1265

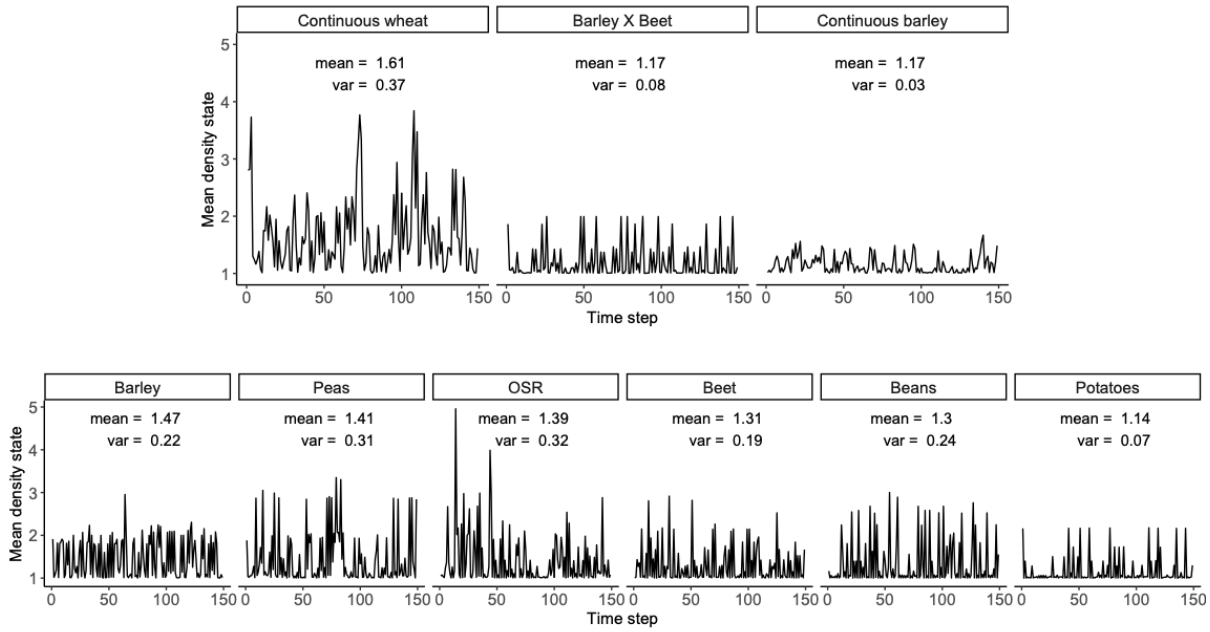

1266

1267

1268

1269

1270

1271

1272

1273

1274

1275

1276

1277

1278

1279

1280

1307

1308

1309

1310

1311

1312

1313

1314

1315

1316

1317

1318

1319

1320

1321

1322

1323

1324

Developing hierarchical density-structured models to study the national-scale dynamics of an arable weed.

Robert M. Goodsell[1] , Dylan Z. Childs[1] , Matthew Spencer[2], Shaun Coutts[3] , Remi Vergnon[1], Tom Swinfield[4], Simon A. Queenborough[5] , Robert P. Freckleton[1].

Submitted to: *Ecological Monographs*.

Methods:

Prior specifications:

In all models , the population-wide effects of source states 2-5, β_{j+1} ... β_J, were drawn from independent normal distributions, with mean 0 and standard deviation 10:

$$\beta_j \sim N(0,10). \qquad \text{(Equation S1)}$$

Unless specifically stated otherwise cut-point parameters were given a wide uniform prior:

$$c \sim unif(0,10). \qquad \text{(Equation S2)}$$

Model II – Field-level intercept.

In model II, the field-level intercept γ_f was drawn from a normal distribution with mean 0 and standard deviation σ_f, where σ_f is the hyper-parameter for the standard deviation, itself drawn from a half-Cauchy distribution with 5 degrees of freedom.

$$\gamma_f \sim N(0, \sigma_f),$$

$$\sigma_f \sim Cauchy\ (0,5). \qquad \text{(Equation S3)}$$

Model III – Field-level source state effects.

The field-level source state effects γ_{jf} were drawn from a multivariate normal prior with dimension 5, for each source state.

$$\gamma_{jf} \sim MVN(\mu, \Sigma), \qquad \text{(Equation S4)}$$

where μ is a vector of K 0s, and Σ is a K-dimensional covariance matrix. We induce a prior on Σ through $\Sigma = S.\Omega.S$ (Barnard, McCulloch and Meng, 2000) where S is the diagonal matrix of the standard deviations of each component of Σ, σ_k, and Ω is the corresponding correlation matrix of Σ. Within Stan this is parameterized in terms of Cholesky decompositions of the covariance matrix for efficiency and numerical stability (Stan development team 2017). Hence, we use the recommended combination of a half-Cauchy prior on the standard deviations and an LKJ prior (Lewandowski, Kurowicka and Joe, 2009) on the Cholesky factor of Ω. Hence if $\Omega = \mathbf{L}\mathbf{L}^{\mathbf{T}}$; $\mathbf{L}$ is the lower-triangular matrix of Ω, and $\mathbf{L}^{\mathbf{T}}$ its transpose,

$$\sigma_k \sim Cauchy\ (0,5),$$

$$\mathbf{L} \sim LKJ(\mathrm{H}). \qquad \text{(Equation S5)}$$

The hyper-parameter (H) in this case is set to 1, which reflects a uniform distribution on the correlation matrix.

Model IV – Field-level cut-points.

For hierarchical cut-points to remain identifiable, it is necessary to ensure that their ordering remains intact, i.e. $c_1 < c_2 < c_3 < c_4$ must be true for a given field. This can be achieved by re-parameterization of the cut-points themselves (Tutz and Hennevogl, 1996; Hartzel, Agresti and Caffo, 2001). The ordering transformation is handled in stan by mapping the ordering constraints onto an unconstrained vector *y*:

$$c_k = \begin{cases} y_1 & \text{if } k = 1, \\ c_{k-1} + \exp(y_k) & \text{if } 1 < k \leq K. \end{cases} \quad \text{(Equation S6)}$$

Group-level cut-points can then be implemented by using hierarchical priors on the parameter space between model cut-points and fixing the first group-level cut-point parameter c_{1f}:

$$c_{1f} \sim N(0,1),$$

$$c_{kf} - c_{k-1f} \sim N(\mu, \sigma). \quad \text{(Equation S7)}$$

The first group-level cut-point, c_{1f}, is given a standard normal prior whilst distances between subsequent cut-points are given normal priors with a mean of μ and standard deviation σ.

The mean for all cut-point distances μ is given a wide normal prior with a mean of 0 and standard deviation of 10. The standard deviation of cut-point distances σ is given a half-Cauchy prior with mean of 0 and 5 degrees of freedom:

$$\mu \sim N(0,10),$$

$$\sigma \sim Cauchy(0,5). \quad \text{(Equation S8)}$$

Model V – Field-level cut-points and field level intercept.

The final model, Model V, is a combination of the above, with both random cut-points and a random intercept included in the linear predictor. As such the linear predictor is the same as in Model II, and the cut-point parameters are the same as in model IV.

All models were fitted using adaptive Hamiltonian MCMC, implemented in Stan version 2.17 (Stan Core Development Team 2017), interfaced with R version 3.4.0 (R Core Development Team 2017) through the package 'Rstan' version 2.17.3 (Stan Core Development Team 2017). Models were run with 4 independent chains over 3000 iterations, each with an additional 1000 iteration warmup period. Trace plots were inspected to assess mixing and potential convergence problems, of which no evidence was found. Calculated scale reduction factors were close to 1, suggesting that the iteration number was providing optimum efficiency. Effective sample sizes were all deemed to be sufficient to provide accurate inference.

Population dynamics under different rotations can be modelled by changing the transition matrix in successive time steps in the Markov model. For example, consider a three-course rotation from crop *A* through crops *B* and *C* back to crop *A* in the fourth year:

$$\mathbf{n}(t+1) = \mathbf{T}_{\mathrm{AB}}\mathbf{n}(t),$$

$$\mathbf{n}(t+2) = \mathbf{T}_{\mathrm{BC}}\mathbf{n}(t+1), \qquad \text{(Equation S9)}$$

$$\mathbf{n}(t+3) = \mathbf{T}_{\mathrm{CA}}\mathbf{n}(t+2),$$

where subscripts on $\mathbf{T}$ denote rotations between specific crops. For example, $\mathbf{T}_{\mathrm{AB}}$ could represent transition probabilities for weed density states between a year in which the crop is wheat and a following year in which the crop is barley, $\mathbf{T}_{\mathrm{BC}}$ transition probabilities under a rotation from barley to oil-seed rape (OSR), and $\mathbf{T}_{\mathrm{CA}}$ transition probabilities under a rotation from OSR back to wheat. Longer rotations can be simulated by extending the number of time steps. More complex rotations can be modelled by changing the order of rotation-specific transition matrices. The only condition is that the destination crop of the previous matrix is the initial crop of the next, i.e. if one matrix models the transitions from wheat to barley, the next matrix in the sequence must model the transitions from barley to the next crop.

The system defined in equation (3) is still a Markovian process, even though the transition matrices vary from year to year. As an example, consider the transition from crop A back to crop A through rotations AB and BC and CA. The density in year 4 can be modelled as a direct function of the density in year 1, without the intermediate steps:

$$\mathbf{n}(t+3) = \mathbf{T}_{\mathrm{CA}}\mathbf{T}_{\mathrm{BC}}\mathbf{T}_{\mathrm{AB}}\mathbf{n}(t) = \mathbf{T}_{\mathrm{ABCA}}\mathbf{n}(t). \qquad \text{(Equation S10)}$$

The model in equation (4) has the same form as equation (1) and also defines a Markovian process (Skellam, 1967), specifically a time-inhomogeneous Markovian process.

Results & discussion:

Posterior predictive checks that compare field-scale error for each density state for OSR-to-wheat and wheat-to-OSR rotations (Figure S1 a and b) demonstrate similar patterns to those for the wheat-to-wheat subset (Figure 3 main text). Non-hierarchical models have much greater errors around all density-state estimations, and hierarchical models display the same order of prediction error, i.e. models with hierarchical cut-points (IV and V) have smaller errors. There are generally larger errors when estimating field-scale densities in the wheat-to-OSR rotation, which may be due to detectability, or ecological factors such as crop density or competition between crop and black-grass. These errors are much smaller, however, in hierarchical models, which highlights advantage of modelling density-structured models in a hierarchical manner.

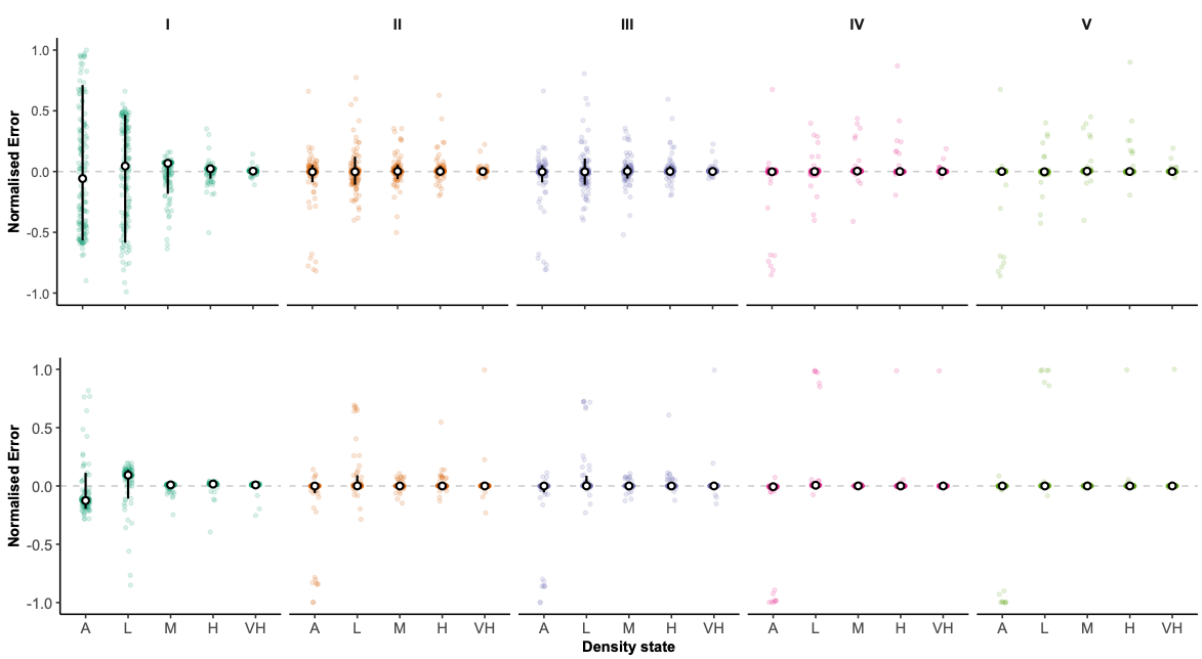

Figure S1. Field-level error between observed and predicted frequencies for each density state category for the wheat to OSR (top row) and OSR to wheat (bottom row) subsets. Hollow dots are median field-scale differences between predicted and observed frequencies of each density state across all fields, vertical bars are 80% equal-tailed credible intervals. Colours represent each of our 5 models, and individual coloured points represent the difference in observed vs density-state frequencies for individual fields.

There is considerable variability in the distribution of within rotation stable density states (Figure S2 a), and damping ratios (Figure S2 b). There were bimodal, or high variance, distributions across multiple rotations for mean density-state and damping ratio. This was most notable in continuous wheat, and wheat rotations broken with OSR, sugar beet, and barley. This suggests that there could be conditions within rotations that lead to two different outcomes of managements; high or low densities. This could be due to factors such as herbicide resistance status, with resistant populations having higher equilibrium densities, or environmental conditions being more favourable at some locations. Alternatively, it could be due to variability in managements such as spring vs winter cropping, where spring of certain crops cropping allows a window to remove weeds from the field before planting of the next crop. This is likely to be the case in wheat rotations broken with sugar beet or barley, which are often cited by farmers as good spring cropping alternatives.

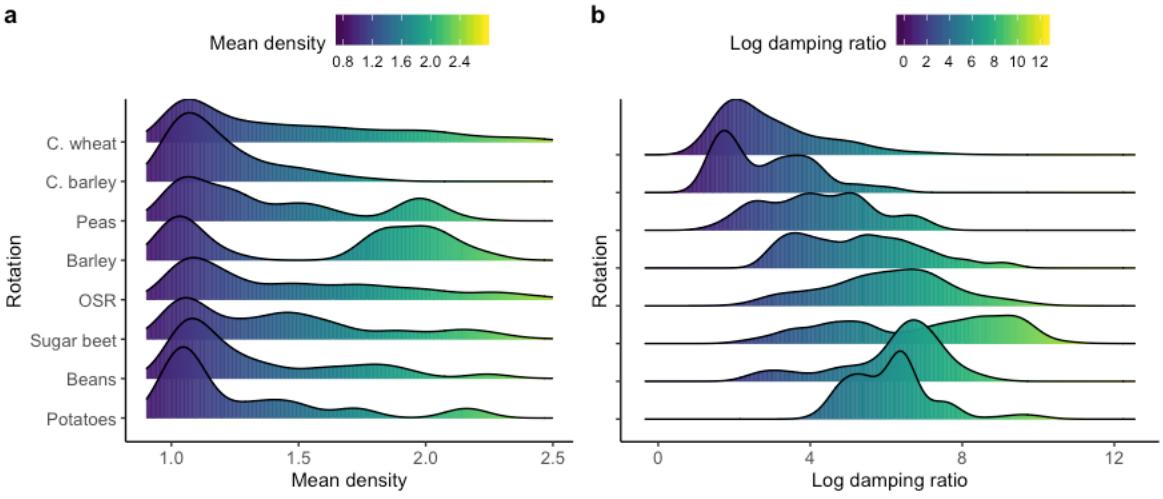

Figure S2. The densities of (a) log of field-scale mean densities and (b) damping ratios for asymptotic & transient analyses of two-step rotations. The colour of each scale represents the corresponding value of each metric.

The relationship between mean equilibrium density-state and damping ratio was also considerably variable within rotations (Figure S3). The pairing of these two metrics is ecologically interesting, as high damping ratios paired with low densities may suggest fast convergence due to low equilibrium population sizes. In rotated systems this could be due to regular perturbation and control of weed populations present in rotated systems. High densities paired with high damping ratios suggest fast convergence on high densities. There is evidence for these dynamics in several rotations, namely continuous wheat, and wheat-to-OSR systems. These dynamics could again be influenced by favourable environmental conditions, herbicide resistance, initial densities and seed bank persistence in a given field, and variability in management. Unpicking the causes of the variability in dynamics that are illustrated by Figures S2 and S3, is an interesting avenue for future research, but will require additional covariate data to be collected on management practices and environmental variables that were unfortunately unavailable for these analyses.

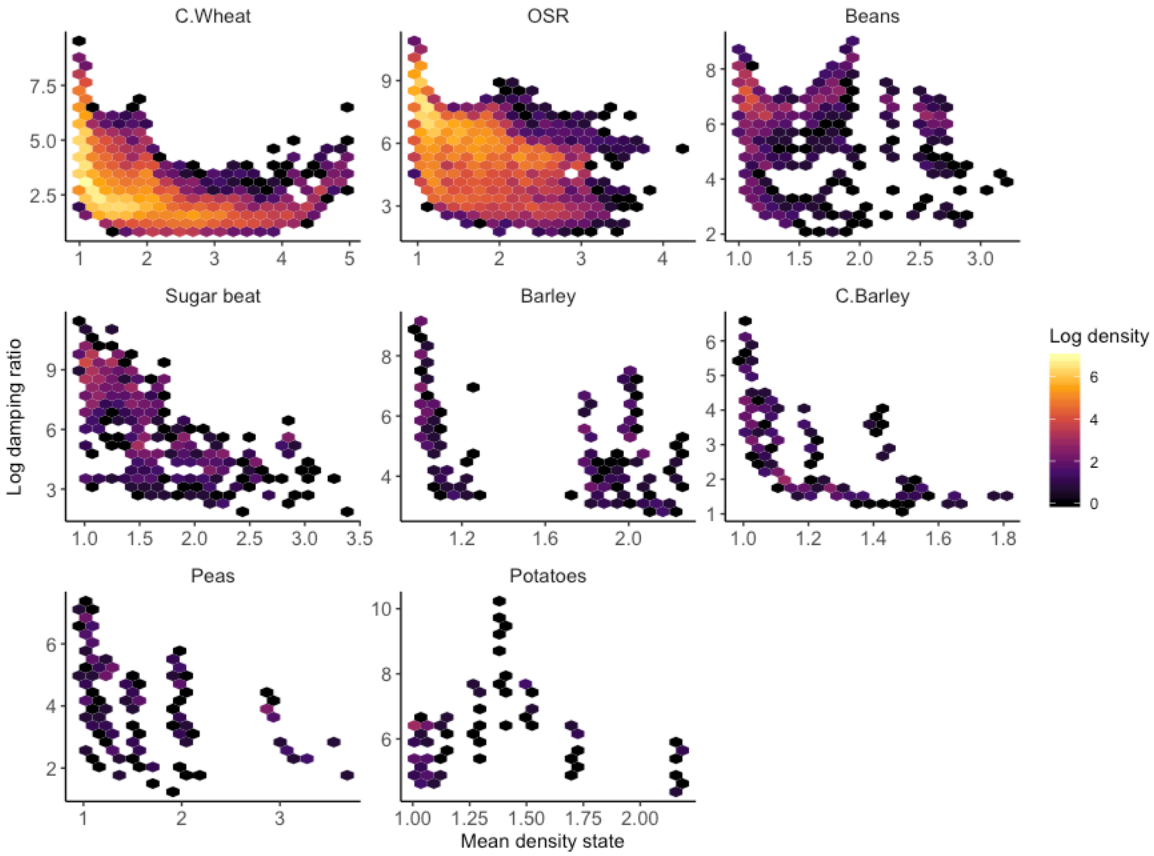

Figure S3. The relationship between damping ratio and the mean density of the stable state distribution of a particular matrix for each rotation in our analyses. The colour of each hex represents the log density of individual matrices at those values.

With regards to management, the effect of cropping strategies on between year variability in weed density is worth consideration (Figure S4). Potatoes produced significantly lower between year variability (Figure S4a), whilst OSR, peas and barley produced the highest levels of between year variability in black-grass densities Potatoes were the only break crop that produced almost consistent negative autocorrelation, and barley and OSR produced consistently positive autocorrelation between years. The implications for rotation specific densities are therefore mixed, the high densities found in barley and OSR are likely to persist, whilst the low densities in potatoes are not. Optimization of controls to account for the periodicity observed in weed densities is a valuable area of future research.

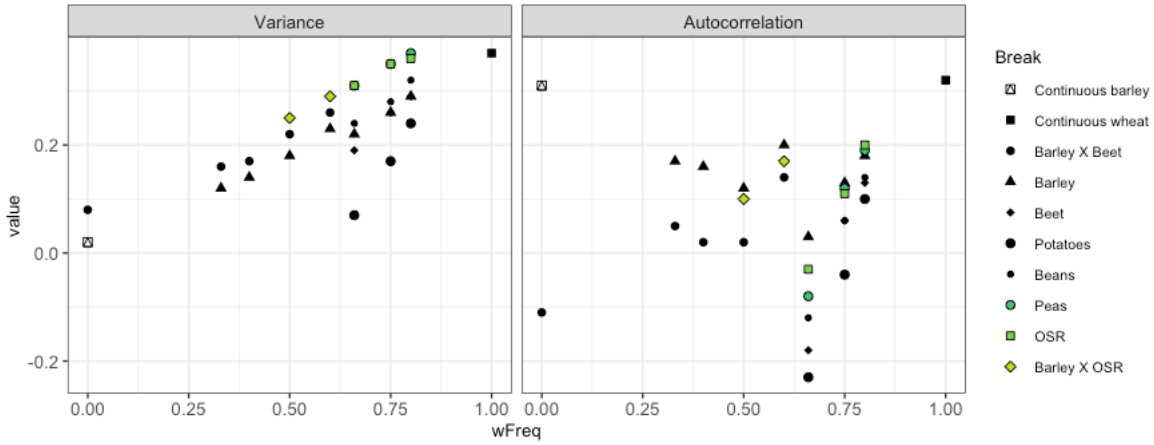

Figure S4. The variance and lag-1 autocorrelation coefficient from stochastic simulations of black-grass density. Individual points represent time-series averages for a model with a specific break crop/rotation at a specific proportion of winter wheat. Colours and shapes of each point represent the break-crop or combination of break crops used in each model.

References

Barnard, J., McCulloch, R. and Meng, X.-L. (2000) 'Modelling Covariance Matrices in Terms of StandardDeviations and Correlations With Applications to Shrinkage', *Statistica Sinica*, 10(4), pp. 1281–1311.

Hartzel, J., Agresti, A. and Caffo, B. (2001) 'Multinomial logit random effects models', *Statistical Modelling: An International Journal*, 1(2), pp. 81–102.

Lewandowski, D., Kurowicka, D. and Joe, H. (2009) 'Generating random correlation matrices based on vines and extended onion method', *Journal of Multivariate Analysis*. Elsevier Inc., 100(9), pp. 1989–2001.

Skellam, J. G. (1967) 'Seasonal periodicity in theoretical population ecology', *Proceedings of the 5th Berkeley Symposium on Mathematics, Statistics, and Probability*, 4, pp. 179–205.

Tutz, G. and Hennevogl, W. (1996) 'Random effects in ordinal regression models', *Computational Statistics & Data Analysis*, 22(5), pp. 537–557.